Available online at www.sciencedirect.com

ScienceDirect

Geochimica et Cosmochimica Acta 125 (2014) 673–693

Geochimica et Cosmochimica Acta

www.elsevier.com/locate/gca

The oceanic mass balance of copper and zinc isotopes, investigated by analysis of their inputs, and outputs to ferromanganese oxide sediments

S.H. Little [a,b,*], D. Vance [a,b], C. Walker-Brown [c], W.M. Landing [d]

[a] Bristol Isotope Group, School of Earth Sciences, University of Bristol, Wills Memorial Building, Queen's Rd, Bristol BS8 1RJ, UK
[b] Institute of Geochemistry and Petrology, Department of Earth Sciences, NW D81.4, Clausiusstrasse 25, 8092 Zürich, Switzerland
[c] School of Environmental Sciences, University of East Anglia, Norwich Research Park, Norwich NR4 7TJ, UK
[d] Department of Earth, Ocean, and Atmospheric Science, Florida State University, 117N. Woodward Ave., Tallahassee, FL, USA

Received 13 February 2013; accepted in revised form 21 July 2013; available online 14 August 2013

Abstract

The oceanic biogeochemical cycles of the transition metals have been eliciting considerable attention for some time. Many of them have isotope systems that are fractionated by key biological and chemical processes so that significant information about such processes may be gleaned from them. However, for many of these nascent isotopic systems we currently know too little of their modern oceanic mass balance, making the application of such systems to the past speculative, at best. Here we investigate the biogeochemical cycling of copper (Cu) and zinc (Zn) isotopes in the ocean. We present estimates for the isotopic composition of Cu and Zn inputs to the oceans based on new data presented here and published data. The bulk isotopic composition of dissolved Cu and Zn in the oceans (δ^{65}Cu ~+0.9‰, δ^{66}Zn ~+0.5‰) is in both cases heavier than their respective inputs (at around δ^{65}Cu = +0.6‰ and δ^{66}Zn = +0.3‰, respectively), implying a marine process that fractionates them and a resulting isotopically light sedimentary output. For the better-known molybdenum isotope system this is achieved by sorption to Fe–Mn oxides, and this light isotopic composition is recorded in Fe–Mn crusts. Hence, we present isotopic data for Cu and Zn in three Fe–Mn crusts from the major ocean basins, which yield δ^{65}Cu = 0.44 ± 0.23‰ (mean and 2SD) and δ^{66}Zn = 1.04 ± 0.21‰. Thus for Cu isotopes output to particulate Fe–Mn oxides can explain the heavy isotopic composition of the oceans, while for Zn it cannot. The heavy Zn in Fe–Mn crusts (and in all other authigenic marine sediments measured so far) implies that a missing light sink is still to be located. These observations are some of the first to place constraints on the modern oceanic mass balance of Cu and Zn isotopes.

1. INTRODUCTION

The isotope systems of the transition metals are increasingly being developed in the Earth Sciences (e.g. Albarède, 2004; Anbar and Rouxel, 2007). The biogeochemistry of these elements suggests two obvious potential applications of their isotope systems in the marine realm. Firstly, many trace metals are well-known to be biologically-active (Bruland and Lohan, 2003; Morel and Price, 2003) so that the attendant isotopic fractionations (e.g. Beard et al., 1999; John et al., 2007a; Navarrete et al., 2011) may have some utility in understanding the detailed processes controlling

* Corresponding author at: Institute of Geochemistry and Petrology, Department of Earth Sciences, NW D81.4, Clausiusstrasse 25, 8092 Zürich, Switzerland. Tel.: +41 44 632 6455.
E-mail address: susan.little@erdw.ethz.ch (S.H. Little).

0016-7037
http://dx.doi.org/10.1016/j.gca.2013.07.046

their biological cycling on the modern and ancient Earth. Secondly, the speciation and oxidation state of the transition metals in the oceans is redox-sensitive, and this is important to their biogeochemical cycling because of the control on the reactivity of the metals concerned, such as their solubility or their susceptibility to scavenging (e.g. Algeo and Maynard, 2008; Helz et al., 2011). Given that speciation and oxidation state changes also induce isotopic fractionations, a second potential application of the new isotope systems is in tracking past ocean redox state. With regard to the latter potential application, most progress has been made with molybdenum isotopes, where the speciation in oxic versus euxinic (free H_2S-bearing) aqueous solutions is fundamentally different, where the rate of output is controlled by this speciation, and where speciation-related isotopic fractionations are imprinted on sediments, both ancient and modern (reviews in: Anbar and Rouxel, 2007; Scott and Lyons, 2012).

However, the Mo isotope system also highlights complexities in using isotope systematics to probe past redox conditions, for example with regard to the intermediate isotopic fractionations observed in both anoxic but non-euxinic (McManus et al., 2006; Poulson et al., 2006; Siebert et al., 2006; Poulson-Brucker et al., 2009; Scott and Lyons, 2012) and mildly euxinic (Nägler et al., 2011) settings. There is a clear need, therefore, to harness the potentially complementary information that may be held in less-developed transition metal isotopic systems. Moreover, though Mo is certainly a biologically-active transition metal, its direct involvement in biology is not quantitatively important to its oceanic biogeochemical cycling (Nakagawa et al., 2012). In contrast it is well-known that biological uptake and regeneration determines Zn depth profiles in the modern ocean (Bruland and Lohan, 2003), and early isotopic data (Bermin et al., 2006; John et al., 2007a; Peel et al., 2009; Zhao et al., in press) hints that this may also be the case for the Zn isotopic system. Copper distributions in the modern ocean are thought to be strongly influenced by both biological recycling and scavenging processes (Bruland and Lohan, 2003), and the first data for Cu isotopes in rivers and oceans has suggested that organic complexes with biologically-produced ligands are an important control on dissolved oceanic isotopic compositions (Vance et al., 2008). It seems likely, therefore, that the isotopic systems of Cu and Zn could be useful in understanding the biogeochemical cycling of these metals in the modern ocean (e.g. Albarède, 2004), with applications to the quantification of key processes in the past ocean through their analysis in sedimentary outputs.

The development of Cu and Zn isotopes as sources of biogeochemical information, however, requires a much better understanding of the modern oceanic isotopic mass balance of these two metals than we currently have. This paper adopts a two-pronged approach to bridging this gap. We present new isotopic data for riverine Zn isotopes, and for both Cu and Zn isotopes in Atlantic marine aerosol, allowing us to summarise the current state of knowledge with respect to the inputs of Cu and Zn to the modern ocean. The main outcome of this, as has already been suggested for Cu isotopes (Vance et al., 2008), is that there must be isotopic fractionation during marine cycling, such that the isotopic composition of Cu and Zn in the dissolved oceanic pool are driven away from the input composition by one or more of the sedimentary outputs. Similar patterns of marine source-sink isotopic fractionation have previously been observed for other metal isotope systems, including Mg and Ca (Tipper et al., 2006, 2010), and the better established transition metal isotope system of Mo, with the isotopic mass balance in this case closed by fractionation during sorption to Fe–Mn oxides (Siebert et al., 2003). In pursuit of an understanding of this issue, then, the second part of this study begins to address the nature of the outputs. Cu and Zn isotopic analyses are reported from the sedimentary record of one of the main sinks, the Fe–Mn crust record of sorption to particulate Fe–Mn oxides. Finally, we assess the implications of the new data for the oceanic mass balance of Cu and Zn and their isotopes.

2. BACKGROUND: THE MARINE BIOGEOCHEMISTRY OF CU AND ZN

The interpretation of much of the isotopic data presented later in this paper will be grounded in what we know of the marine chemistry of Cu and Zn, so before proceeding to those data we first present a short review of the most important aspects of that marine chemistry, which will serve as a template for the interpretation of the isotopic data.

Copper and Zn are both strongly cycled between the surface ocean and the deep (e.g. Boyle et al., 1977b; Bruland, 1980). Zn concentrations in the deep Atlantic and Pacific are around 2 and 10 nM respectively (e.g. Bruland, 1980; Bruland and Franks, 1983; Bruland et al., 1994; Boyle et al., 2012), but are often <0.1 nM in the photic zone (e.g. Bruland, 1980; Lohan et al., 2002). The strong depletion of Zn in the surface ocean has been attributed to biological uptake (e.g. Morel and Price, 2003), with regeneration in the deep ocean driving up concentrations. Zn concentration profiles, however, exhibit deeper regeneration maxima than the major labile nutrients and closely resemble those of dissolved silica (e.g. Bruland, 1980). Copper concentration profiles also show surface depletion and deep enrichment but, whereas the deep/surface concentration ratio can be several hundred for Zn, it is never more than about 5–10 for Cu. In addition, depth profiles for Cu are also much more linear than those of both Zn and the major nutrients (e.g. Boyle et al., 1977b; Bruland, 1980; Martin et al., 1993). Bruland and Lohan (2003) attribute this to the particle reactivity of Cu, and the importance of scavenging (in addition to biological recycling) in controlling dissolved Cu distributions.

A key aspect of the dissolved chemistry of both Cu and Zn is organic complexation. Copper is well-known to be strongly complexed to organic ligands (e.g. Coale and Bruland, 1988; Moffett and Dupont, 2007) such that $<0.1\%$ of the total dissolved fraction (operationally-defined as passing through a 0.2 or 0.4 μm filter) is free Cu^{2+}. Culture experiments have shown that the ligands that bind Cu are produced by a range of phytoplankton groups, including cyanobacteria (Moffett and Brand, 1996; Croot et al.,

1999, 2000; Gordon et al., 2000), dinoflagellates and diatoms (Croot et al., 1999, 2000), and coccolithophores (Leal et al., 1999; Croot et al., 2000; Dupont et al., 2004; Dupont and Ahner, 2005), thought to be a response to the toxicity of the free Cu^{2+} ion. Two studies of the distribution of the Cu-binding ligands with depth (Coale and Bruland, 1988; Moffett and Dupont, 2007) report conflicting results – with one concluding that the ligands were restricted to the upper North Pacific water column and another that they are present throughout the same water column. The latter finding is inconsistent with the suggestion that the ligands are actively produced by phytoplankton, unless they are very refractory and long-lived. Recent data supports the finding that Cu-binding ligands are persistent throughout the water column, though further work is required to corroborate this observation in a wider range of geographical settings (e.g. Buck et al., 2012). Zinc is also dominantly complexed to organic ligands in seawater (e.g. Bruland, 1989; Donat and Bruland, 1990), though perhaps to a slightly lesser extent than Cu and by rather weaker ligands. In the case of Zn, it is suggested that these ligands are produced by cell lysis upon death (Ellwood and Van den Berg, 2000), and that they reduce Zn^{2+} to near-limiting levels in the photic zone (Bruland and Lohan, 2003).

The behaviour of Cu and Zn is very different in settings where O_2 levels in the water column are low to zero (anoxic), or where H_2S is a significant dissolved constituent (euxinic) (Jacobs et al., 1985, 1987; Haraldsson and Westerlund, 1991; Tankéré et al., 2001). In the deep Black Sea where total sulphide levels reach a few 100 μM, for example, Cu and Zn are almost completely stripped out of solution and are correspondingly enriched in sediment (Calvert, 1990; Haraldsson and Westerlund, 1991). We know little about the precise chemistry by which aqueous concentrations are lowered and transfer to sediment occurs, however (e.g. Jacobs et al., 1987; Calvert and Pedersen, 1993). Copper and Zn enrichments in anoxic sediments are probably controlled by both sulphidisation (e.g. Black Sea) and transfer of organic matter to the sediment (e.g. Francois, 1988; Calvert and Pedersen, 1993; Brumsack, 2006; Tribovillard et al., 2006).

3. SAMPLES AND METHODS

3.1. Samples, sample selection and preparation

The aim of this paper is to improve our understanding of the oceanic mass balance of Cu and Zn isotopes in the ocean. This first requires knowledge of the isotopic composition of the inputs of Cu and Zn to the oceans. Vance et al. (2008) published a dataset for the Cu isotopic composition of the dissolved phase of large and small rivers. We supplement this here with Zn isotopic data for a subset of these rivers. The details of the samples and their collection can be found in Vance et al. (2008) and Archer and Vance (2008). Briefly, all river samples were collected from close to the bank, into cleaned, low density polyethylene bottles after pre-rinsing with the sample 2–3 times. The Amazon, Brahmaputra, Nile and Chang Jiang samples were immediately passed through a pre-cleaned cellulose nitrate 0.2 μm filter using a pre-cleaned plastic filter holder and reservoirs, pre-rinsed with filtered sample before final filtrate collection, then decanted into a new cleaned low density polyethylene bottle. The Kalix, Missouri and Tocantins samples were filtered in the same manner up to 2 weeks after collection, on return to the laboratory. For these latter samples, there is some potential for sorption of Zn to bottle surfaces, and therefore isotopic fractionation (Fischer et al., 2007; Schlosser and Croot, 2008; Fitzsimmons and Boyle, 2012). We note, however, that these samples encompass the full spread of Zn concentrations and Zn isotopic compositions of the dataset. All samples were acidified to pH 2 after filtration with concentrated twice-distilled HCl. All river samples were pre-concentrated prior to column chromatography and mass spectrometry (see Section 3.2) by drying down, treatment with concentrated nitric acid (containing a small amount of H_2O_2) to oxidise organics, and re-dissolution in a few ml HCl.

There are also no published data for the Cu–Zn isotopic composition of aerosol delivered to the surface ocean, likely the other main source to the oceans apart from rivers (Chester and Jickells, 2012). We also present new data for Atlantic marine aerosol samples that derive from the CLIVAR/CO_2 Repeat Hydrography section A16N. Sample collection details were published previously (Buck et al., 2010). Briefly, aerosols were collected for 24 h on a pre-cleaned 0.45 μm, 47 mm diameter polypropylene filter atop a 7 m aluminium tower mounted forward of the bridge and away from the ships infrastructure. The data here are for de-ionized water soluble Cu and Zn, obtained by leaching a filter for 10 s with 100 ml de-ionized water (pH 5.6), as described in detail in Buck et al. (2010) for "DI soluble analyses". This approach was chosen by Buck et al. (2010) to mimic conditions an aerosol would encounter during wet deposition, a process thought to comprise 50–90% of global aerosol Fe deposition to the oceans. Approximately 50–80 ml of the leach solution was obtained from Florida State University and pre-concentrated as above for the river samples.

We also present Cu and Zn isotope data for one of the major sedimentary outputs from the oceans, hydrogenetic Fe–Mn crusts. These Fe–Mn crusts are used as a proxy for the sorptive output to dispersed particulate Fe–Mn oxides found throughout sediments deposited under oxic conditions in the modern ocean. They form by pure hydrogenetic precipitation on hard-rock substrates of mid-plate volcanic edifices, at water depths of 400–4000 m (Hein et al., 1997). Exactly how they grow is not completely understood, but the process is very slow: growth rates vary between 1 and 10 mm/Ma (Koschinsky and Hein, 2003). They grade into Fe–Mn crusts with a strong hydrothermal influence (whose formation occurs via direct precipitation from hydrothermal plumes close to vents), and are distinct from Fe–Mn nodules, which are abyssal plain deposits forming by a combination of hydrogenetic and diagenetic processes (Hein et al., 1997). Copper and Zn isotope data for a global dataset of Fe–Mn *nodules* have been previously published by Albarède (2004) and Maréchal et al. (2000), who report average values of $\delta^{65}Cu = 0.31 \pm 0.23‰$ and $\delta^{66}Zn = 0.90 \pm 0.28‰$ respectively (Maréchal et al., 2000; Albarède, 2004).

Three Fe–Mn crust samples were analysed, one from each of the major ocean basins. The three crusts are:

1. D11-1 from the central Pacific: 11°38.9N, 161°40.5E, water depth ~1.8 km.
2. Alvin 539 2-1 (referred to as herein as Alv539) from the New England Seamount in the northwest Atlantic: 35°36N, 58°47W, water depth ~2.7 km.
3. 109D-C from the Madagascar Basin, SW Indian Ocean: 28°S, 61°E, water depth 5.2–5.7 km.

Age and growth rate data for all three Fe–Mn crusts have been previously calculated from $^{10}Be/^{9}Be$ ratios, and vary between 1.4 and 2.7 mm/Myr for D11-1 (Ling et al., 1997). 109D-C has a growth rate of 1.55 mm/Myr and Alv539 2.37 mm/Myr (O'Nions et al., 1998). Growth rates were estimated assuming that Fe–Mn crusts have grown with the same $^{10}Be/^{9}Be$ ratio as measured at their present-day surface.

Depth profiles for isotopic analysis were carried out using a New Wave Research Micromill with Brasseler diamond scriber mill bit, each Fe–Mn crust sampled eight times at regularly spaced intervals. Lines of 1 mm length and 1 mm depth were scribed and each sample (as fine particulate) was collected and dissolved in 0.4 M hydrochloric acid.

3.2. Analytical methods for Cu–Zn concentration and isotopic analysis

The acids and reagents used in this study, all Merck AnalaR grade reagents, were further purified by single, or double sub-boiling distillation in Teflon stills. 18.2 MΩ grade water was obtained from an 18.2 MΩ (MQ) water purification system. All work was carried out under clean laboratory conditions in ISO5 clean hoods, utilising only trace-metal cleaned Savillex PFA labware.

All samples for isotopic analysis were first analysed for concentrations of Cu, Zn and other relevant solutes on a Finnigan Element 2, single collector, fast scanning magnetic-sector ICPMS at the Bristol Isotope Group, University of Bristol. This latter analysis was done on a small aliquot of the solutions obtained as described above, and before column chemistry to purify Cu and Zn for isotopic analysis. Concentrations were calculated using a primary artificial elemental standard, prepared in house. A commercially available river water reference material for trace metals was used as a secondary standard, to assess accuracy and reproducibility of the elemental analyses (SLRS-5, National Research Council Canada). For Cu the long-term reproducibility of this standard is ±9% (2 RSD, $n = 46$), and the average Cu concentration obtained is 103% of the certified value. For Zn, the reproducibility for SLRS-5 is ±14%, and the average Zn concentration is 94% of the certified value. For one Element run (of a total of twelve considered) during which data for the Indian (109D-C) and Pacific (D11-1) Fe–Mn crusts were collected, Zn concentrations for both SLRS-5 and another secondary standard were 80% of their certified values. The Zn reproducibility estimate quoted here thus excludes standard data from this run, and analysed Zn concentrations for these two Fe–Mn crusts were scaled up accordingly before calculation of Zn/Al and Zn/Mn ratios. For Mn and Al, reproducibility of the SLRS-5 standard is ±13% and ±10% respectively, and their measured concentrations are 100% and 104% of the certified values.

The Cu and Zn fractions of all samples were purified by ion exchange chemistry using a strongly basic anion resin (Bio-Rad macroporous AG MP-1M Resin), as detailed in Maréchal et al. (1999) and refined in Archer and Vance (2004). Two column passes were performed on all samples. The purified Cu was oxidised to eliminate residual organics by refluxing overnight in $HNO_3 + H_2O_2$. Following a last dry-down and re-dissolution in around 1 ml 2% HNO_3, final element concentrations for analysis were ~100 ppb Cu, and 100–200 ppb Zn. Isotope values were measured using a ThermoFinnigan Neptune high-resolution multicollector ICPMS (in low mass resolution mode), with samples introduced in around 1 ml 2% nitric acid via a CPI PFA nebuliser (50 μl/min) attached to a glass spray-chamber for Cu (the Stable Introduction System made by Elemental Scientific Inc, Omaha, NE, USA) or an Aridus desolvating nebuliser system (Cetac, Omaha, NE, USA) for Zn. All Cu and Zn isotope analyses were collected in static mode using a multiple Faraday collector array. Data collection consisted of 30 4 s integrations and each measurement was preceded by an analysis (15 4 s integrations) of the 2% HNO_3 used to make up the analyte solutions. These "on-peak zeroes" were then subtracted from the sample signals. In all cases they amount to no more than 0.02% of the analyte beam. Sensitivities for Cu were typically 1.5–2 V on ^{63}Cu at 100 ppb total Cu, and 15–20 V on ^{64}Zn at 400 ppb Zn. Zinc isotope data in this study are reported relative to the Johnson Matthey (JMC) Zn standard solution, from the Lyon-CNRS laboratory. Mass bias correction for Zn was achieved using a ^{64}Zn–^{67}Zn double spike with spike-sample ratios of ~1 (detailed procedure in: Bermin et al., 2006). Mass bias on the Neptune is very stable, too stable for the application of a (e.g. Zn) doping approach for Cu, and thus Cu data were obtained by simple standard bracketing with analyses of pure, un-treated NIST SRM 976 and are reported relative to this standard. This approach has been demonstrated to produce high-quality Cu isotope data (e.g. Zhu et al., 2000; Mason et al., 2004; Bermin et al., 2006; Vance et al., 2008). Both Cu and Zn ratios are given in the standard delta per mil notation:

$$\delta^{65}Cu = \left[\frac{(^{65}Cu/^{63}Cu)_{sample}}{(^{65}Cu/^{63}Cu)_{NIST976}} - 1\right] \times 1000 \quad (1)$$

$$\delta^{66}Zn = \left[\frac{(^{66}Zn/^{64}Zn)_{sample}}{(^{66}Zn/^{64}Zn)_{JMC-Lyon}} - 1\right] \times 1000 \quad (2)$$

All uncertainties cited are 2 sigma unless stated otherwise. Long-term reproducibility of Cu data was monitored by analysis of a secondary pure Cu standard solution (supplied by A. Matthews, Hebrew University, Jerusalem) run against SRM976, with $\delta^{65}Cu = 0.11 \pm 0.11‰$ ($n = 102$) over a period of 30 months between November 2009 and May 2012, and compared with $0.10 \pm 0.06‰$, measured at the Hebrew University (Asael et al., 2007). Verification of

the Zn double spike method is carried out by the analysis of mixtures of the double spike with JMC-Lyon standard during every analytical session, for which the predicted isotopic fractionation is zero, as per the definition of δ^{66}Zn. The result for the period of this study and for mixtures with std/spike ratios in the range 0.1–2.0 was $\delta^{66}Zn = 0.03 \pm 0.08‰$ ($n = 170$).

4. RESULTS

4.1. Rivers

The new Zn isotope data for rivers are presented in Table 1 and displayed against reciprocal Zn concentrations, to explore mixing relationships, in Fig. 1. Overall, dissolved riverine Zn isotopic compositions show a range in δ^{66}Zn of 1‰, from −0.12‰ (Tocantins at Belem) to +0.88‰ (Kalix, Gallivare sample), and a range of Zn concentrations from 3 (Kalix) to 46 nM (Brahmaputra). Samples from individual rivers sometimes show relatively tight groupings (e.g. Chang Jiang), while samples from along the very large Amazon system (including two large tributaries, the Negro and Solimoes) spread across the entire dataset. The Blue and White Nile were sampled in both dry and wet season, and while there may be systematically higher concentrations in the wet season (but only two data points), Zn isotope values are not very different for the two sampling periods. While the data in Fig. 1 do not show a strong correlation between Zn isotope values and reciprocal Zn concentrations ($R^2 \approx 0.3$), we calculate a Pearson prod-

Table 1
Zn concentrations and isotopic compositions in selected world rivers.

River	Sample	[Zn] nM	δ^{66}Zn[a] ‰	River averages:		Water discharge[b] (10^{12} l/year)	Zn discharge (moles/year)
				[Zn] nM	δ^{66}Zn[a] ‰		
Kalix	Gallivare	8.2	0.88				
	Abgesa	5.2	0.60				
	Kamlunge	12.5	0.37				
	Kalix	2.7	0.57				
	Kalix	4.2	0.80	6.6	0.64	9	5.9×10^4
White Nile (wet)	Wad Madani, Sudan	37.5	0.04				
White Nile (dry)	Wad Madani, Sudan	9.8	0.17				
Blue Nile (dry)	Rabak, Sudan	44.3	0.31				
Blue Nile (wet)	Rabak, Sudan	6.6	0.29				
Main Nile (dry)	Shendi, Sudan	19.0	0.30				
Main Nile (dry)	Aswan, Egypt	10.2	0.23				
Main Nile (dry)	Cairo, Egypt	38.1	0.19				
Main Nile (dry)	Luxor, Egypt	45.6	0.13	26.4	0.21	83	2.2×10^6
Chang Jiang	15 km upstream of Wuhan	11.6	0.52				
	15 km upstream of Wuhan	13.5	0.83				
	15 km upstream of Wuhan	10.8	0.46				
	15 km upstream of Wuhan	10.9	0.64				
	Wuhan	16.5	0.37	12.7	0.56	928	1.2×10^7
Solimoes (Amazon)	Manaus	5.0	0.55				
Negro (Amazon)	Manaus	24.7	0.43				
Negro (Amazon)	Manaus	18.5	0.48				
Negro (Amazon)	Manaus	12.7	0.12				
Tocantins	Belem	32.4	-0.12				
Tocantins	Belem	17.4	0.04				
Tocantins	Belem	32.0	0.18				
Amazon	Belem	11.8	0.57				
Amazon	Belem	4.4	0.61				
Amazon	Belem	18.7	0.38				
Amazon	Belem	17.1	0.36	17.7	0.33	6590	1.2×10^8
Missouri	Columbia, Missouri	39.0	0.19				
	Columbia, Missouri	40.3	0.41	39.7	0.30	580	2.3×10^7
Brahmaputra	Tezpur, Assam	45.8	0.31	45.8	0.31	1003	4.6×10^7
Sums and averages	Discharge- and [Zn]-weighted average:				0.33	9193	2×10^8
Scale-up to global discharge						38000	8.3×10^8

Note that discharge given for Missouri is for the entire Mississippi system, that for the Brahmaputra is for the entire Ganges–Brahmaputra system and that for the Ottawa is for the entire St. Lawrence system.

[a] All internal errors (within-run uncertainty given as 2SE) are less than the reproducibility as estimated from multiple analyses of standards (0.08‰ for Zn and 0.11‰ for Cu).

[b] Discharges as in Gaillardet et al. (1999) and Pontér et al. (1990).

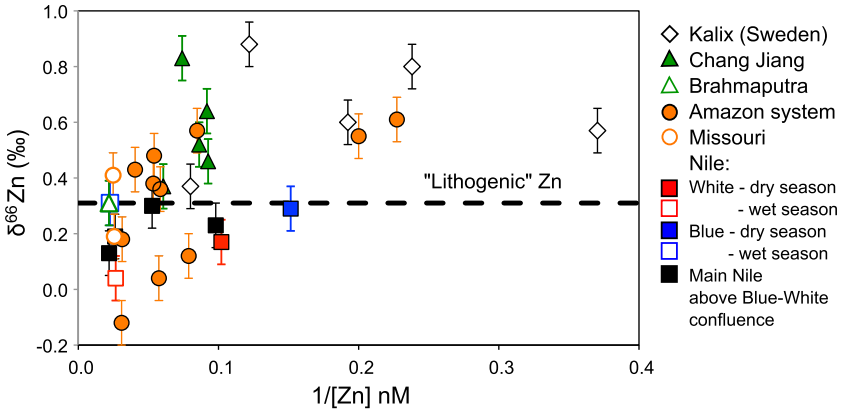

Fig. 1. Zn isotope data for rivers, plotted against reciprocal Zn concentration. Symbols shown in key. Dashed line gives the Zn isotopic composition of "lithogenic" Zn, i.e. Zn in rocks and sediments from the continents that are dominated by silicate material (data compiled in Electronic Supplementary Table). Error bars are reproducibility on Zn isotope measurements (2SD = 0.08‰).

Table 2
Zn and Cu abundances and isotopic compositions of the water leachable fraction of Atlantic marine aerosols.

Date	Latitude[a]	Longitude	Zn (ng)[b]	δ^{66}Zn (‰)[c]	2 Sigma	Cu (ng)	δ^{65}Cu (‰)	2 Sigma
06/25/07	54.50	−20.00	57	0.38	0.08	1.4		
06/29/07	47.11	−20.00	102	0.41	0.08	6.6		
07/03/07	40.50	−20.00	219	0.26	0.08	21	0.04	0.11
07/04/07	38.95	−20.00	101	0.17	0.08	6.3		
07/10/07	30.69	−21.70	58	0.13	0.08	1.6		
07/21/07	24.45	−26.50	102	0.18	0.08	1.5		
07/22/07	22.95	−27.34	47	0.49	0.08	0.8		
07/23/07	21.06	−28.40	80	0.37	0.08	9.5		
07/26/07	16.33	−29.00	60	0.26	0.08	12	0.06	0.11
07/27/07	15.00	−29.00	81			17	0.30	0.11
07/28/07	13.37	−29.00	105	0.26	0.08	5.2		
07/29/07	11.66	−29.00	34	0.30	0.08	16		
08/01/07	7.45	−27.22	198	0.52	0.08	11	−0.18	0.11
08/02/07	5.67	−26.34	92	0.51	0.08	4.0		
08/03/07	3.99	−25.50	315	0.54	0.08	23	−0.05	0.11
08/04/07	2.33	−25.00	256	0.50	0.08	22	−0.16	0.11
08/05/07	0.97	−25.00	164	0.49	0.08	6.1		
08/06/07	−0.36	−25.00	103	0.45	0.08	10		
Average and 1 SD					0.37	0.14	0.00	0.18

[a] Start latitude (+ = N) and longitude (− = W) for start of aerosol collection. Collection for 24 h.
[b] Amount of Zn (and Cu) in nanograms retrieved by leaching a 47 mm filter (that accumulated aerosol for 24 h) with 100 ml of DI water for 10 s. Corrected for blank filter treated with the same procedure. Blank contribution to total measured Zn was around 20% on average. For Cu it was around 11% on average.
[c] Zn and Cu isotopic compositions not corrected for filter blank as this was too small to measure. Quoted uncertainties on Zn and Cu isotopic compositions are the reproducibilities of the respective standards.

uct-moment correlation coefficient of $\rho = 0.53$ and critical value of $p \approx 0.002$, indicating that the correlation is significant at the 99.8% level. There is thus a general tendency for rivers with low Zn concentrations to display the heaviest Zn isotope values.

4.2. Atlantic marine aerosol

Isotope data for the instantly soluble Cu and Zn obtained from Atlantic marine aerosols are presented in Table 2, and displayed against latitude in Fig. 2. The approximate source of the aerosols at each latitude (from air mass back trajectory analysis presented in Buck et al., 2010) is also shown. Zinc isotope compositions show minor but analytically significant variation (δ^{66}Zn = +0.13 to +0.54‰) both above and below the average value for data for silicate-dominated sediments and rocks from the continents (Fig. 2, "lithogenic" Zn, data compiled in Electronic Supplementary Table). The average and 1SD for the entire dataset is δ^{66}Zn = +0.37 ± 0.14‰, indistinguishable from the average lithogenic value. There is enough resolution on Fig. 2 to note that data for aerosols with a source in central Africa (collected between the Equator and about 7°N) are significantly heavier (δ^{66}Zn = 0.49–0.52‰) than the litho-

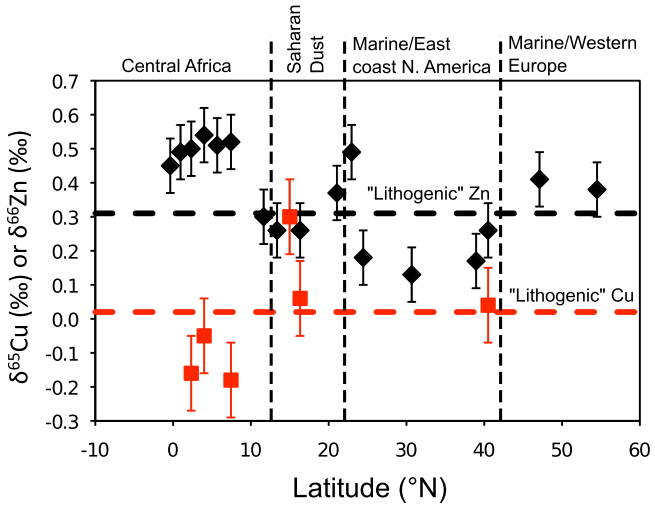

Fig. 2. Zn (black) and Cu (red) isotopic data for the water soluble fraction of marine aerosol from the Atlantic Ocean (the CLIVAR/CO_2 Repeat Hydrography section A16N). Error bars are the 2 sigma reproducibility for Zn and Cu isotopic measurements reported herein (0.08‰ for δ^{66}Zn and 0.11‰ for δ^{65}Cu). Horizontal dashed lines give the Zn (black) and Cu (red) isotopic compositions of "lithogenic" Zn and Cu i.e. Zn and Cu in rocks and sediments from the continents that are dominated by silicate material (data compiled in Electronic Supplementary Table). Vertical dashed lines give the approximate sources of the aerosol, as calculated in Buck et al. (2010) using air-mass back trajectories. (For interpretation of the references to color in this figure legend, the reader is referred to the web version of this article.)

genic value. Taken as a set, these samples also contain the highest contents of leachable Zn. Data from 24 to 41°N, sourced from the eastern coast of North America, may be slightly lighter than the lithogenic value (δ^{66}Zn = 0.13–0.26‰). All the other data, including dust from the Sahara, plot more or less within uncertainty of the lithogenic value. Data for Cu isotopes are too sparse (due to Cu contents that were generally too low for isotopic analysis, see Table 2) to identify systematic variation, and δ^{65}Cu = varies from −0.18 to +0.30‰. As for Zn isotopes, the average and 1 SD, at δ^{65}Cu = 0.00 ± 0.18, is indistinguishable from the lithogenic average (Fig. 2, lithogenic data compiled in the Electronic Supplementary Table).

4.3. Ferromanganese crusts

Data for three Fe–Mn crust samples, representative of one of the main sedimentary sinks for Cu and Zn from the oceans, are presented in Table 3 and displayed against ^{10}Be-derived age in Fig. 3. As observed for previously published Fe–Mn crusts (Shimmield and Price, 1986; Manheim and Lane-Bostwick, 1991), their average Mo/Mn ratio is 0.002. Cu/Mn and Zn/Mn ratios exhibit more scatter, likely due to the non-conservative distribution of these two elements in ocean waters (Bruland and Lohan, 2003). The mean Cu/Mn ratio for our three Fe–Mn crusts is 0.004, and the Zn/Mn ratio is 0.003, comparable to global mean values calculated from a USGS compilation of published Fe–Mn crust analyses (Cu/Mn 0.005, Zn/Mn 0.004) (Manheim and Lane-Bostwick, 1991).

For the three Fe–Mn crusts δ^{65}Cu ranges between −0.16 and 1.19‰, representing accumulation of Fe–Mn oxides over the past 19 Ma. Over the same period, δ^{66}Zn ranges between +0.60 and +1.13‰. Within these ranges, however, there is structure in the data when taken together with metal/Al ratios and the enrichment factor of Cu and Zn in the Fe–Mn crusts relative to average shale (Wedepohl, 1991) (Table 3). Note that enrichment factors are calculated after normalization to the Al content of the sediment (Al is used as a tracer for the lithogenic fraction of the element of interest) and relative to a reference material, usually 'average shale' as analysed by Wedepohl (1991), as follows:

$$EF_{\text{element X}} = \frac{(X/Al)_{\text{sample}}}{(X/Al)_{\text{average shale}}} \quad (3)$$

The Pacific sample (D11-1) shows virtually no variation in Cu and Zn isotope values outside of analytical uncertainty for the past 17 Ma, with a mean δ^{65}Cu value of 0.54 ± 0.07‰ and a mean δ^{66}Zn of 1.12 ± 0.12‰. This homogeneity in Cu and Zn isotopic composition is associated with high Cu/Al and Zn/Al ratios (Table 3), and high enrichment factors for both elements (Fig. 4). The Atlantic Fe–Mn crust (Alv539) isotopic values are slightly more variable, but also relatively uniform for the 15 Ma period spanned by this sample, with a mean δ^{65}Cu of 0.33 ± 0.15‰ and δ^{66}Zn = 0.96 ± 0.17‰. The Atlantic crust has lower Cu/Al and Zn/Al ratios and lower enrichment factors than D11-1 (Table 3, Fig. 4). In general, the Indian Ocean sample (109D-C) has isotope values that are more variable still, alongside low enrichment factors for both Cu and Zn. δ^{65}Cu values for the Indian Ocean crust decrease from +0.3 to +0.15 between 11 and 6 Ma ago, and remain relatively low (at δ^{65}Cu ≈ 0.15‰) from this point forward, while Zn isotope values are generally similar to the Fe–Mn crusts from the other two oceans. The Indian Fe–Mn crust is also characterized by outlying analyses – including one very heavy Cu isotopic composi-

Table 3
Summary of ferromanganese crust Cu and Zn geochemistry, including enrichment factors (calculated relative to average shale (Wedepohl, 1991) and isotope ratios.

Crust	Sample	Depth in crust mm	Age Ma	Cu/Mn	Zn/Mn	Mo/Mn	Cu/Al	Zn/Al	EF Cu	EF Zn	$\delta^{65}Cu$[a] ‰	$\delta^{66}Zn$[a] ‰
Alvin 539 – Atlantic	539-A	2	0.8	0.003	0.004	0.003	41.7	45.3	15.5	9.2	0.27	1.06
	539-B	6	2.5	0.001	0.001	0.001	53.1	62.4	19.7	12.6	0.37	1.00
	539-C	10.5	4.4	0.000	0.000	0.000	54.2	60.9	20.1	12.3	0.37	1.04
	539-D	16	6.8	0.004	0.005	0.003	43.4	53.1	16.1	10.8	0.40	0.95
	539-E	21	8.9	0.004	0.005	0.003	40.5	45.2	15.0	9.2	0.32	0.93
	539-F	26	11.0	0.005	0.006	0.003	41.5	50.2	15.4	10.2	0.24	0.94
	539-G	30.5	12.9	0.004	0.004	0.003	39.3	41.4	14.6	8.4	0.25	0.80
	539-H	36	15.2	0.004	0.003	0.003	51.8	43.3	19.2	8.8	0.44	1.00
Average:				0.003	0.003	0.002	45.7	50.2	17.0	10.2	**0.33**	**0.96**
109D-C – Indian	I1	2.5	1.6	0.003	0.002	0.002	32.2	23.0	12.0	2.2	0.15	0.95
	I2	6.5	4.2	0.004	0.002	0.002	31.7	16.8	11.8	1.6	0.13	1.08
	I3	9.5	6.1	0.004	0.002	0.002	42.0	20.3	15.6	1.9	0.12	0.98
	I4	13	8.4	0.005	0.002	0.002	23.8	12.9	8.8	1.2	0.23	*1.42*
	I5	17	11	0.005	0.003	0.002	16.8	9.6	6.2	0.9	0.31	1.03
	I6	20.5	13.2	0.006	0.004	0.002	13.4	8.8	5.0	0.8	*−0.16*	0.80
	I7	25	16.1	0.005	0.003	0.002	13.8	8.0	5.1	0.8	0.27	*0.60*
	I8	30	19.3	0.007	0.007	0.001	10.4	10.1	3.8	0.9	*1.19*	1.01
Average:				0.005	0.003	0.002	23.0	13.7	8.5	1.3	**0.20**	**0.97**
D11-1 – Pacific	P1	2	1.5	0.002	0.002	0.002	94.6	128.3	35.1	12.0	0.48	1.13
	P2	7	5.1	0.003	0.003	0.002	96.3	79.9	35.8	7.5	0.55	1.08
	P3	12.5	8	0.003	0.002	0.002	157.1	133.0	58.3	12.4	0.57	1.11
	P4	15	8.9	0.004	0.003	0.002	121.6	91.9	45.1	8.6	0.58	1.06
	P5	19.5	10.6	0.004	0.002	0.002	156.7	91.1	58.1	8.5	0.51	1.06
	P6	27	13.4	0.005	0.003	0.002	349.6	191.3	129.7	17.9	0.58	1.23
	P7	30.5	14.7	0.005	0.003	0.002	318.3	173.6	118.1	16.2	0.52	1.19
	P8	37.5	17.3	0.006	0.003	0.002	231.1	134.0	85.8	12.5	0.53	1.09
Average:				0.004	0.003	0.002	190.7	127.9	70.8	12.0	**0.54**	**1.12**

Bold text drawing attention to average isotope values.
[a] Outlying isotope ratios in italics are discussed further in the text. All internal errors (within run uncertainty given as 2SE) are less than the reproducibility (0.08‰for Zn and 0.11‰for Cu)

tion at 19 Ma and one very light at 13 Ma, as well as less extreme outliers in Zn isotopic composition to both lower and higher values.

5. DISCUSSION

5.1. River and aerosol data: natural and anthropogenic controls

It is not our purpose here to analyse the data for the inputs and their controls in detail, but merely to present them as the best estimate we currently have of the likely isotopic composition of the inputs as a parameter in the oceanic mass balance. However, some discussion of the data is required in order to establish the degree to which these small datasets might be representative of global inputs, and in particular whether there is likelihood of any bias due to either natural or anthropogenic processes.

The data for Zn isotopes in rivers, when plotted against reciprocal Zn concentrations (Fig. 1), display a characteristic that is reminiscent of data previously reported for dissolved Cu and Mo in rivers (Archer and Vance, 2008; Vance et al., 2008): that there is a positive correlation (in the case of Zn very weak) between the isotopic composition and the reciprocal Zn concentration. In the case of Cu and Mo this correlation was ascribed to the partitioning of heavy isotopes into the dissolved phase, and light isotopes into particulate phases, during weathering and transport. Aside from the weakness of the correlation for Zn there is one other important difference. In the case of Mo and Cu the dissolved load of the rivers has $\delta^{98}Mo$ or $\delta^{65}Cu$ that are universally heavier than the lithogenic value. For Zn the data spread above and below the lithogenic value, suggesting more complex processes whose identity is very difficult to narrow down with these data.

The high $\delta^{66}Zn$ in the Kalix system, in the Chang Jiang and in some Amazon samples might be ascribed to the contribution from the weathering of a carbonate end-member given the high $\delta^{66}Zn$ measured in carbonates (Pichat et al., 2003), but there is no carbonate in the Kalix catchment and the Amazon catchment represents a very diverse mix of lithologies. Thus it seems probable that the heavier Zn isotopes paired with generally lower concentrations are controlled by the same retention of the light isotope in the particulate phase during weathering and transport as seen for Cu and Mo. In this view, and as with the latter two elements, more quantitative weathering leads to release of more Zn that is closer in isotopic composition to the rock that is weathering. The broad array in Fig. 1 would then be a complicated product of

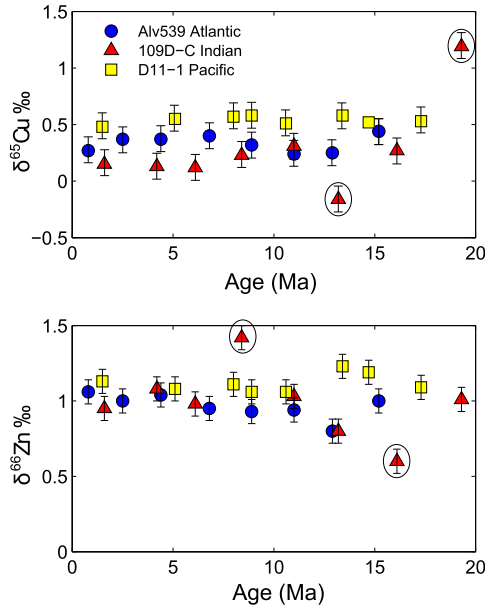

Fig. 3. Top: Measured Cu isotope values, and Bottom: Measured Zn isotope values for three ferromanganese crusts. Cu isotope values vary between 0.1‰ and 0.5‰, and are relatively uniform in time. Zn values are very homogeneous, at ca. 1‰. Circled anomalous values are discussed further in the text, and in Fig. 4.

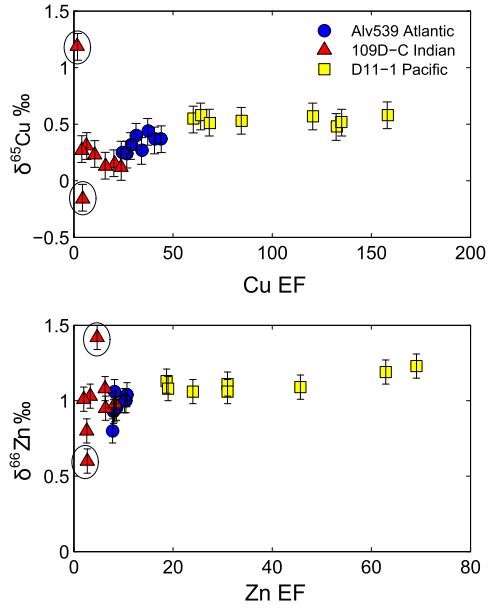

Fig. 4. Cu (upper panel) and Zn (lower panel) isotope values for the three ferromanganese crust samples, plotted against metal enrichment factors (calculated as per Eq. (3)). The latter points to the detrital component of the crust, with high enrichment factors indicating high levels of authigenic enrichment. The anomalous isotope values circled in Fig. 3 are shown here to be those at low levels of authigenic enrichment.

this process, in combination with another process that produces high Zn concentrations and isotopic compositions lighter than the lithogenic Zn isotope composition (the lower end of the array in Fig. 1).

A significant worry for the purposes of this study is that this second process, resulting in the isotopically lighter end of the array in Fig. 1, is an anthropogenic source of Zn to rivers. When considering steady state oceanic mass balance it is necessary to exclude any anthropogenic component to the present oceanic inputs, which are insignificant on the timescale of the Zn oceanic residence time. It is highly probable that these rivers are anthropogenically-contaminated to some extent, but it is very difficult to establish the impact of this on riverine Zn isotopic compositions. One study of anthropogenic Zn observed that most common forms fall in the δ^{66}Zn range of 0.1–0.3‰ (John et al., 2007b), while in another, isotopically light values in the highly polluted River Seine were attributed to the leaching of Parisian rooftops (Chen et al., 2008). For the purposes of this study it is significant, however, that the main Amazon stem sampled at its mouth at Belem, where anthropogenic contamination is likely to be at its peak, is no different in isotopic composition from the samples of the Solimoes and Negro tributaries obtained much further upstream at Manaus. The Amazon system dominates the estimate of the δ^{66}Zn of the riverine input to the oceans that can be obtained from the data in Table 1, of δ^{66}Zn = +0.33‰. This might be viewed as a problem in itself, in that there is a danger of non-representativeness, but the Amazon data as a set certainly spread along much of the entire riverine dataset so this seems unlikely. The part of the lower Amazon system that is significantly different, with δ^{66}Zn below the lithogenic value, is the Tocantins (Table 1), but if the three data for the Tocantins at Belem are omitted from the calculation of the average in Table 1, that average is shifted upwards by only 0.05‰.

While there is potential that the removal of the anthropogenic contribution to rivers might shift the average δ^{66}Zn upwards slightly, for the aerosol data the opposite may be the case. The data that stand out in Fig. 2 are those from latitudes just north of the Equator with δ^{66}Zn = 0.45–0.54‰, for which the dust is sourced in central Africa. Buck et al. (2010) suggested that excesses of V and Mn over Ti in these samples points to a significant anthropogenic contribution. High oxalate contents (Landing, unpublished data) in these samples might suggest a contribution from biomass burning. In the only published study of δ^{66}Zn in urban aerosols, however, Cloquet et al. (2006) report isotopically light values from the polluted Metz region of France (at δ^{66}Zn = 0.12‰; Cloquet et al., 2006). Regardless, for our purposes in using these data to estimate oceanic inputs this issue is barely significant: dust is likely to be a minor part of the input relative to rivers (see Section 6.1), and removal of the low latitude data from Table 2 would shift the calculated isotopic composition of the input (δ^{66}Zn = 0.33‰, see Section 6.1) to the oceans by less than 0.01‰.

5.2. Cu and Zn isotopes in Fe–Mn crusts: systematics and controls

Some of the variation in Zn/Al, Cu/Al and Zn and Cu enrichment factors in the Fe–Mn crust samples reported in this study may be due to real differences in accumulation rates of Cu and Zn, perhaps associated with differing deep

ocean Cu and Zn concentrations in the various ocean basins. For example, the greater enrichment in Cu and Zn in the Pacific relative to the Atlantic sample is qualitatively consistent with higher deep ocean Cu and Zn concentrations in the Pacific versus the Atlantic (e.g. Bruland, 1980; Martin et al., 1993). However, enrichment factors in the Indian Ocean Fe–Mn crust are very low. In this case metal/Al ratios are up to an order of magnitude lower than those in the other two Fe–Mn crusts (Table 3) and the resultant low enrichment factors are associated with much greater variability in the Cu and Zn isotopic compositions (Fig. 4). Even for the Atlantic Fe–Mn crust, the only Zn isotopic analysis that is different from any of the others beyond analytical error is the one with the lowest Zn enrichment factor (at 12.9 Ma). Low authigenic enrichments increase the significance of analytical artifacts in isotope measurements and, more importantly, introduce the possibility of contamination from phases other than the targeted Fe–Mn oxyhydroxides. Thus, we consider that the isotopic data for the Pacific and Atlantic samples (bar the single Zn isotopic analysis mentioned for the Atlantic crust) is likely to robustly reflect the isotopic composition of Cu and Zn sorbed to Fe–Mn oxides in these two ocean basins, while the low enrichments in the Indian Ocean Fe–Mn crust render this data rather suspect. The averages for data from the Atlantic and Pacific crusts are thus $\delta^{65}Cu = 0.44 \pm 0.23‰$, and $\delta^{66}Zn = 1.04 \pm 0.21‰$ (mean and 2 SD).

We note that the data summarized for Cu and Zn isotopes in Fe–Mn crusts overlap with those for Fe–Mn nodules ($\delta^{65}Cu = 0.31 \pm 0.23‰$ (Albarède, 2004); $\delta^{66}Zn = 0.90 \pm 0.28‰$ (Maréchal et al., 2000)). It thus seems highly likely that these data, taken together, are representative of the output of dissolved Cu and Zn from the oceans via sorption to Fe–Mn oxides. This being so, the Cu isotopic composition of this output is about 0.4–0.6‰ lighter than the deep ocean dissolved pool (Vance et al., 2008; Boyle et al., 2012; Thompson et al., 2013), while its Zn isotopic composition is 0.5–0.6‰ heavier than dissolved Zn in the deep oceans (Boyle et al., 2012; Zhao et al., in press). Our main concern here is the implications of these data for the oceanic mass balance of Cu and Zn isotopes, and an assessment of the precise mechanisms driving these isotopic separations are beyond the scope of this paper. However, we note in passing that these data are consistent with the explanation put forward in Vance et al. (2008) for the heavy dissolved pool of Cu in the oceans. These authors suggested that dissolved Cu in the oceans was driven towards heavy values due to equilibrium partitioning of the isotopes between the organic-ligand-bound Cu in the dissolved phase and sorption to particulate Fe–Mn oxides. The strength of the bonds holding Cu in these organic complexes would favour the preferential incorporation of the heavy isotope. The reasons for the fact that Zn shows the opposite sense of fractionation are less clear. While Zn is also complexed in the oceanic dissolved pool, these complexes are apparently less strong (Bruland and Lohan, 2003; Yang and Van den Berg, 2009). Therefore, it may be that the equilibrium isotope partitioning between dissolved and sorbed Zn is closer to that expected for free Zn in the dissolved phase, or a weak inorganic ligand. In this latter case the data for Fe–Mn crusts are perhaps consistent with experiments involving inorganically-speciated Zn in the aqueous phase, which show that the heavy Zn isotopes almost always sorb more readily (Pokrovsky et al., 2005; Juillot et al., 2008; Balistrieri et al., 2008).

6. SYNTHESIS: IMPLICATIONS FOR THE OCEANIC MASS BALANCE OF CU AND ZN AND THEIR ISOTOPES

In this final section, we review the data presented in this study, and their associated uncertainties, within the framework of a quantitative estimate of the oceanic mass balance of Cu and Zn and their isotopes. Oceanic mass balance can be considered in two ways. Firstly, it can be evaluated in terms of a simple elemental flux mass balance calculation. For example, Rehkamper and Nielsen (2004) carry out an analysis of the oceanic mass balance of thallium (-Tl-), based purely on their best estimates of Tl fluxes into and out of the ocean. At steady state, the elemental flux into the ocean is equal to the flux out to sediment:

$$F_{in} = F_{out} \tag{4}$$

Where F_{in} represents the sum of all the known input fluxes, and F_{out} represents the sum of the known output fluxes. If the known fluxes in are different from the known fluxes out, and the system is assumed to be in steady state, it is possible to assess the magnitude of any missing source or sink. Given knowledge of the total mass (M) of the element of interest in the ocean, it is also possible to calculate an oceanic residence time (τ_{res}) for the element:

$$\tau_{res} = \frac{M}{F_{in}} \equiv \frac{M}{F_{out}} \text{ (at steady state)} \tag{5}$$

Secondly, additional constraints on oceanic mass balance can be established by a calculation of an element's isotopic mass balance, such as that attempted for $\delta^{26}Mg$ by Tipper et al. (2006). The equation governing the rate of change of the isotopic composition of an element in seawater (δ_{sw}) is:

$$\frac{dM_X\delta_{sw}}{dt} = F_{in}\delta_{in} - F_{out}\delta_{out} \tag{6}$$

Where M_X is the number of moles of element X in the ocean. In this case, the steady state scenario (i.e. constant δ_{sw}) can be envisaged as follows:

$$F_{in}\delta_{in} = F_{out}\delta_{out} \tag{7}$$

And the isotopic composition of any missing source/sink can be evaluated. The results of our analysis for Cu and Zn are summarised in Tables 4 and 5 respectively, and illustrated schematically in Fig. 5. This is the first attempt to carry out such an exercise for Cu and Zn, and is a useful means to highlight gaps in our current knowledge, and avenues for future research.

Table 4
Fluxes and isotopic compositions (as δ^{65}Cu) of dissolved Cu into and out of the oceans, and oceanic residence times calculated using these flux values.

	Mass (kg)	Ref	Cu concentration		Ref		Mass (mol)	Cu isotopic composition (‰)		Ref
			Range	Best estimate				Range	Best estimate	
Global oceans	1.35×10^{21}	1	0.5–6 nmol/kg	3.1 nmol/kg	2, 5		4.2×10^{12}	+0.7 to +1.2	**+0.90**	18, 21
Input fluxes	Mass flux,	Ref	Cu concentration		Ref	Cu flux (mol/year)		Cu isotopic composition (‰)		Ref
	Best estimate		Range	Best estimate		Range	Best estimate	Range	Best estimate	
Rivers	3.74×10^{16} kg/y	3	5.7–127 nmol/kg	19.3 nmol/kg	4,18,19	$6.0 \times 10^{8} - 8.7 \times 10^{8}$	7.2×10^{8}	+0.02 to 1.45	+0.68	18
Hydrothermal fluids	3.0×10^{13} kg/y	6	na	na			na	nd	nd	
Aerosol dust	4.5×10^{14} kg/y	7		28 ppm 0.44 μmol/kg	8	5.4×10^{7} (Solubility: 27%, ref 9)	5.4×10^{7}	−0.18 to +0.3	0.00	23
Input total						$6.5 \times 10^{8} - 9.2 \times 10^{8}$	**7.7×10^{8}**		**+0.63**	
Residence time (total input)						*4.5–6.4 ky*	*5400 year*			
Output fluxes	Mass flux,	Ref	Cu concentration		Ref	Cu flux (mol/year)		Cu isotopic composition (‰)		Ref
	Best estimate		Range	Best estimate		Range	Best estimate	Range	Best estimate	
Oxic sediments:										
Fe–Mn oxides	*Mo: 9×10^{7} mol/year	10	–	Cu/Mo ratio: 3.6	12	–	4.9×10^{8}	+0.05 to 0.60	+0.31	22, 23
Carbonates	1.1×10^{13} mol/year	11	0–0.2 μmol Cu/mol Ca	0.1	20	$0.0–2.2 \times 10^{6}$	1.1×10^{6}		nd	
Output total							**4.9×10^{8}**		**+0.31**	
Projected missing sink, assuming steady state:							**2.8×10^{8} mol/year**		**+1.19‰**	

Bold text drawing attention to average fluxes and isotopic compositions.

Table 5
Fluxes and isotopic compositions (as δ^{66}Zn) of dissolved Zn into and out of the oceans, and oceanic residence times calculated using these flux values.

	Mass (kg)	Ref	Zn concentration		Ref		Mass (mol)	Zn isotopic composition (‰)		Ref
			Range	Best estimate					Best estimate	
Global oceans	1.35×10^{21}	1	0.1–10 nmol/kg	5.4 nmol/kg	2		7.3×10^{12}		**+0.51**	14
Input fluxes	Mass flux,	Ref	Zn concentration		Ref	Zn flux (mol/year)		Zn isotopic composition (‰)		Ref
	Best estimate		Range	Best estimate		Range	Best estimate	Range	Best estimate	
Rivers	3.74×10^{16} kg/year	3	0.6–96 nmol/kg	15.8 nmol/kg	4, 23	$3.5 \times 10^{8} - 8.3 \times 10^{8}$	5.9×10^{8}	+0.19 to 0.56	+0.33	23
Hydrothermal fluids	3.0×10^{13} kg/year	6	na	na			na	0.00 to +1.04	+0.24	15
Aerosol dust	4.5×10^{14} kg/year	7		67 ppm 1.02 μmol/kg	8	6.9×10^{7} (Solubility: 15%, ref 9)	6.9×10^{7}	+0.13 to 0.54	+0.37	23
Total						$4.2 \times 10^{8} - 9.0 \times 10^{8}$	$\mathbf{6.6 \times 10^{8}}$		**+0.33**	
Residence time (total input)						*8–17ky*	*11,000 year*			
Output fluxes	Mass flux,	Ref	Zn concentration		Ref	Zn flux (mol/year)		Zn isotopic composition (‰)		Ref
	Best estimate		Range	Best estimate		Range	Best estimate	Range	Best estimate	
Oxic sediments:										
Fe–Mn oxides	*Mo: 9×10^{7} mol/year	10	–	Zn/Mo ratio: 2.4	12	–	3.1×10^{8}	+0.53 to 1.42	+0.90	16, 23
Carbonates	1.1×10^{13} mol/year	11	1.4–4.4 μmol Zn/mol Ca	3	13	$1.5 \times 10^{7} - 4.8 \times 10^{7}$	3.3×10^{7}	+0.32 to 1.15	+0.91	17
Total							$\mathbf{3.5 \times 10^{8}}$		**+0.90**	
Projected missing sink, assuming steady state:							**3.1×10^{8} mol/year**		**−0.30‰**	

References for Tables 4 and 5: 1, Baumgartner et al. (1975); 2, Chester and Jickells (2012); 3, Berner and Berner (1996); 4, Gaillardet et al. (2003); 5, Bruland and Lohan (2003); 6, Elderfield and Schultz (1996); 7, Jickells et al. (2005); 8, Rudnick and Gao (2003); 9, Desboeufs et al. (2005); 10, Morford and Emerson (1999), McManus et al. (2006); 11, Milliman et al. (1999); 12, Manheim and Lane-Bostwick (1991); 13, Marchitto et al. (2000); 14, Bermin et al. (2006), Vance et al. (2012), Boyle et al. (2012), Zhao et al. (in press), John et al. (2008); 16, Maréchal et al. (2000); 17, Maréchal et al. (2000); 18, Vance et al. (2008); 19, Boyle et al. (1977b); 20, Boyle (1981); 21, Boyle et al. (2012); Thompson et al. (2013); 22, Albarède (2004); 23, This study. Other points of note: "na" = not applicable – used in reference to hydrothermal fluids, for which quantitative removal is assumed close to the vent source. "nd" = not done. Note that inclusion of "carbonates" within the oxic sediments does not preclude carbonate deposition in reducing environments. *"Mo:" in the mass flux column for output to Fe–Mn oxides is the estimate made by Morford and Emerson (1999) for Mo output to oxic sediments, and is used in combination with Cu/Mo or Zn/Mo ratios to estimate Cu and Zn output to Fe–Mn oxides (see text). Cu/Mo and Zn/Mo ratios given for output fluxes are by weight.

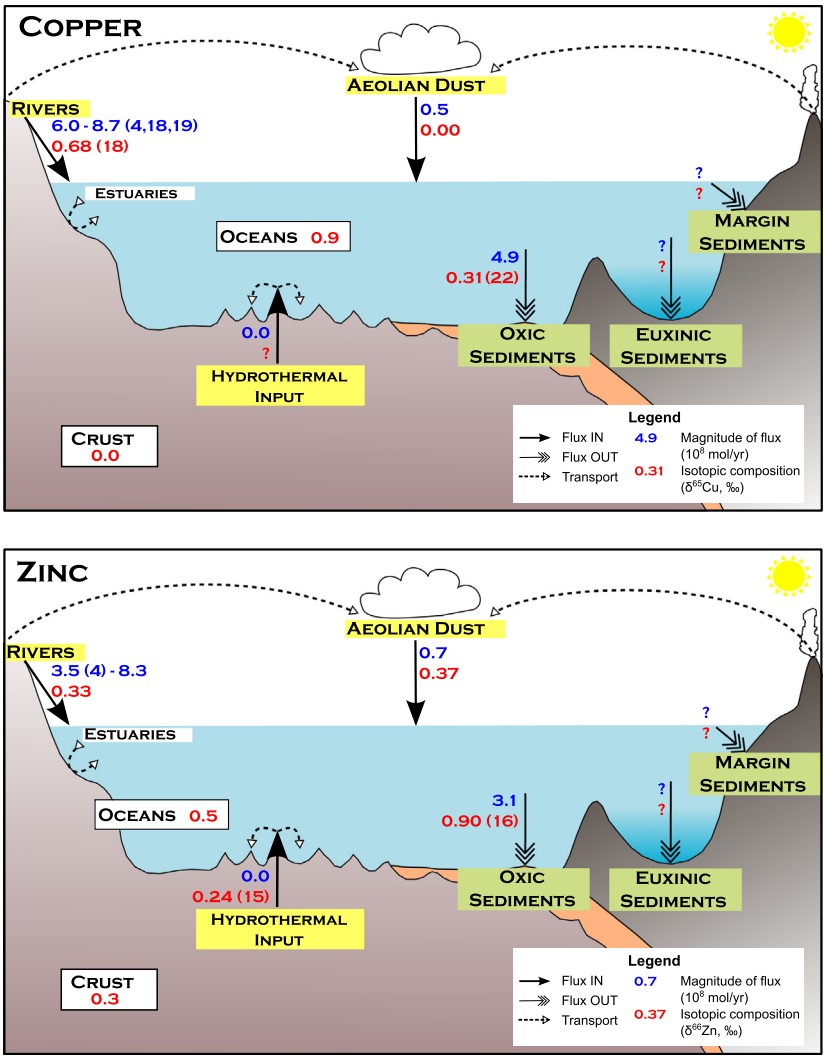

Fig. 5. Schematic diagrams illustrating the global ocean isotopic mass balance of Cu (upper) and Zn (lower), as presented in this study. Data shown are as outlined in this study for the major inputs ("Rivers" and "Aeolian Dust"), and for one of the principal outputs ("Oxic sediments", here represented by isotopic data from Fe–Mn nodules, with fluxes calculated as described in the text). Flux estimates are in blue, and are $\times 10^8$ mol year^{-1} Cu or Zn. Isotopic compositions are in red, in ‰. Other data sources as given in Tables 4 and 5: (4) Gaillardet et al. (2003), (15) John et al. (2008), (16) Maréchal et al. (2000), (18) Vance et al. (2008) (19) Boyle et al. (1977b), (22) Albarède (2004). (For interpretation of the references to color in this figure legend, the reader is referred to the web version of this article.)

6.1. The flux and isotopic composition of the inputs of Cu and Zn to the oceans

The main inputs of both Cu and Zn to the oceans are likely to be from rivers and dust (Chester and Jickells, 2012). There have been no indications thus far of a significant hydrothermal source, so that the sizeable inventories of hydrothermal fluids must be precipitated or scavenged quantitatively very close to vents (Cave et al., 2002; German et al., 1991, 2002; Trocine and Trefry, 1988). Though there are clear caveats involved in using modern measurements of rivers and aerosols as estimates of the inputs to the oceans, some of which are discussed herein, these are the only data we currently have with which to make this estimate.

6.1.1. The riverine flux

Rivers are a key means of trace metal delivery to the oceans. The calculation of an element's riverine input to the oceans is achieved via a simple multiplication of its average dissolved riverine concentration by the estimated total riverine discharge to the oceans (e.g. Gaillardet et al., 1999), for which a value of ~38,000 km^3 year^{-1} is typically used (Berner and Berner, 1996). Accurate data for trace elements in river waters are sparse, however, due to inaccurate historical analyses (Bruland and Lohan, 2003). In addition, anthropogenic input of trace metals, both directly into aquatic systems and via polluted dust deposition, dominates the natural input in some cases (Nriagu and Pacyna, 1988; Shiller and Boyle, 1985). The use of only relatively 'pristine' river analyses in calculating

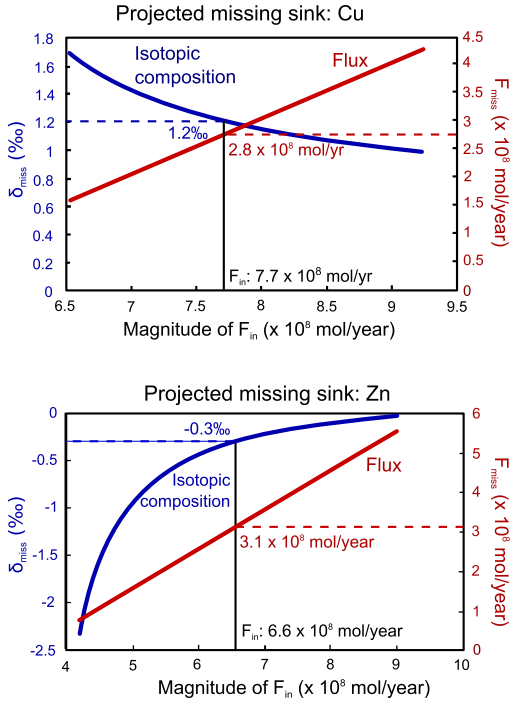

Fig. 6. Models illustrating the sensitivity of the flux and isotopic composition of the projected missing sinks for Cu (upper panel), and Zn (lower panel) given a changing oceanic Cu or Zn input flux. The input flux is in each case assumed to have a fixed isotopic composition (of $\delta^{65}Cu = +0.63‰$ or $\delta^{66}Zn = +0.33‰$). The output flux to oxic sediments is also fixed, with a magnitude for Cu of 4.9×10^8 mol/year and isotopic composition of $\delta^{65}Cu = +0.31‰$, and magnitude for Zn of 3.1×10^8 mol/year and isotopic composition of $\delta^{66}Zn = +0.90‰$. In each figure, the vertical black line intersects the modelled missing flux and its isotopic composition as predicted by the best estimates for Cu and Zn given in Tables 4 and 5 respectively, and the numbers superimposed on each figure reflect these best estimates for the missing sinks. Increasing the magnitude of the input flux increases the magnitude of the missing sink whilst reducing the extremity of its isotopic composition. Conversely, reducing the size of the missing sink renders its isotopic composition more extreme.

a global flux leads to a bias towards rivers predominantly draining tropical ecosystems (in Africa and South America, for example; Gaillardet et al., 2003). This is due to a shortage of sampling in Asia and the Far East, and the existence of relatively few pristine rivers in Western Europe and North America.

Additional uncertainty in the riverine flux occurs due to estuarine processing at the river–sea interface. While the major elements, such Na^+, K^+, Ca^{2+}, and SO_4^{2-}, often exhibit simple conservative mixing (e.g. Chester and Jickells, 2012), the behaviour of trace metals in estuaries is variously controlled by salt-driven flocculation, coagulation and particulate settling (Benoit et al., 1994; Windom et al., 1988; Zwolsman et al., 1997), by the degradation of colloidal material, by biological productivity (Balls, 1990), or by mobilization of Fe and Mn in reducing sediments (Feely et al., 1986). Trace elements may either be removed or remobilized in estuarine environments, or both, reflecting changes in salinity and pH. Colloidal iron particles are largely lost from estuarine and coastal waters due to salt-induced coagulation and particulate settling (Boyle et al., 1977a), and hence very little riverine sourced Fe reaches the open sea (Poulton and Raiswell, 2002). Both conservative and non-conservative behaviour have been reported for Cu and Zn, in a spectrum of estuaries with different hydrodynamic properties (see Ackroyd et al., 1986, and references therein). Mid-salinity maxima are frequently, though not always, observed (cf. Kraepiel et al., 1997; Tang et al., 2002; Wang and Liu, 2003), and have been accounted for by oxidation or deflocculation of organic colloid–metal complexes (Jones and Turki, 1997), remobilization of bottom sediments (Ackroyd et al., 1986), or benthic fluxes from pore-waters (Peterson et al., 1995). Dissolved minima in Cu and Zn have also been observed within the low salinity, high turbidity region, indicating varying degrees of removal particularly in polluted estuaries (Ackroyd et al., 1986). Studies of the estuarine dynamics of two very large rivers (the Amazon and Chang Jiang) report near conservative behaviour for Cu, however (Boyle et al., 1982; Edmond et al., 1985). The riverine flux estimates reported in Tables 4 and 5 assume conservative behaviour of Cu and Zn in estuaries.

Gaillardet et al. (2003) report a mean riverine dissolved input of Cu of 8.7×10^8 mol year^{-1}. Boyle et al. (1977b) estimate the riverine dissolved Cu input at 6×10^8 mol year^{-1}, and Vance et al. (2008) report a similar value of 7×10^8 mol year^{-1}. For the purpose of estimating mass balance in this study, an average dissolved fluxes of 7.2×10^8 mol year^{-1} Cu is assumed (Table 4). For Zn, Gaillardet et al. (2003) report mean a riverine dissolved input of 3.5×10^8 mol year^{-1}. In the new set of Zn analyses presented in this study, for a sub-set of the rivers analysed for Cu in Vance et al. (2008), we estimate the riverine flux of Zn to be a factor of two higher than this Gaillardet et al. (2003) estimate, at 8.3×10^8 mol year^{-1}. An average of 5.9×10^8 mol year^{-1} Zn is thus assumed (Table 5).

Dissolved Cu in a set of large and small rivers analysed by Vance et al. (2008) has a discharge-weighted average $\delta^{65}Cu$ of +0.68‰ ($n = 29$), heavier than the average of the small dataset for igneous rocks and silicate sediments of the continental crust, at around 0‰ ($\delta^{65}Cu = 0.02 \pm 0.15‰$, 1SD, $n = 42$, for the data compiled in the Electronic Supplementary Table). A similarly small dataset for $\delta^{66}Zn$ in rocks suggests that the silicates of the bulk continental crust are around +0.3‰ ($\delta^{66}Zn = +0.31 \pm 0.11‰$, 1SD, $n = 55$, for the data compiled in the Electronic Supplementary Table). Here we report data for the dissolved pool of world rivers that suggests a discharge-weighted average $\delta^{66}Zn$ for the riverine flux of 0.33‰, the same as the lithogenic value.

6.1.2. The dust flux

A second important likely source of Cu and Zn to the oceans is aerosol dust. Dust deposition to the ocean has been estimated in two key ways. First, via measurement based extrapolations from ground and satellite-based observations (e.g. Duce and Tindale, 1991; Prospero et al., 2002), and second, via modelling studies (e.g. Tegen and Fung, 1995). Both approaches have yielded broadly

similar results, although all estimates are to some degree tuned against field data (Mahowald et al., 2005; Jickells et al., 2005). A composite estimate presented by Jickells et al. (2005) compares reasonably well with sediment trap data, however (Kohfeld and Harrison, 2001). They estimate total global dust emissions of 1790 Mt year^{-1}, with 26% of these emissions deposited in the oceans (ca. 450 Mt year^{-1}) (Jickells et al., 2005). Mahowald et al. (2005) estimate uncertainties on the various approaches used to estimate dust fluxes to be on the order of a factor of ten, due to the spatial and geographic variability in dust sources and deposition patterns.

The ocean dust flux is well constrained, however, compared to the chemistry and solubility of trace elements in mineral aerosols. This is because it is not the dust flux that is important, *per se*, but rather the soluble portion of the trace metal of interest. Mineral aerosol research to date has predominantly focused on Fe. The Fe content of dust is usually assumed to be that of the mean crustal composition, at ca. 3.5% (Taylor and McLennan, 1985). The fractional solubility of Fe has been estimated at anywhere between 0.01 and 80%, however, with no general consensus on the most relevant methodology (e.g. Hand et al., 2004; Boyd and Ellwood, 2010). Jickells and Spokes (2001) estimate average Fe solubility of 2% based on measurements made directly in the ocean, similar to estimates of Al solubility of 1.5–3.5% (Gehlen et al., 2003; Measures and Vink, 2000). Aerosol solubility for Cu and Zn is thought to be somewhat higher than for Fe, though studies that report very high values (of up to 70%) are likely recording an anthropogenic dust source (Chester et al., 1994; Chen et al., 2006). Desboeufs et al. (2005) consider the solubility of trace metals in five different aerosols types which form two major groupings, "silicate" and "urban" (or anthropogenic, with a carbonaceous matrix). Leaching was carried out for 120 minutes in pH4.7 MilliQ water to represent atmospheric waters (i.e. rain), and thus simulating wet deposition. In silicates, they find solubility for Cu of 27% (cf 75–98% Cu solubility in "urban" aerosols) and solubility of Zn of 11–19% (cf 99–100% for the "urban" type). Wet deposition is estimated to predominate over dry deposition by a factor of 2:1 (Raiswell and Canfield, 2012). Solubility of Cu and Zn during dry deposition is likely to be somewhat lower that these estimates for silicates, and they therefore place an upper limit on the input of soluble Cu and Zn to the oceans via mineral aerosol.

Using the Jickells et al. (2005) dust deposition estimate of 450 Mt year^{-1}, and Cu and Zn contents of average continental crust of 28 ppm Cu and 67 ppm Zn (Rudnick and Gao, 2003), we calculate total Cu and Zn dust fluxes to the ocean of 2.0×10^8 mol year^{-1} Cu and 4.6×10^8 mol year^{-1} Zn. Assuming 27% dissolution of Cu, the calculated soluble dust flux is thus 5.4×10^7 mol year^{-1} Cu. For 15% dissolution of Zn, the equivalent flux is 6.9×10^7 mol year^{-1} Zn.

The isotopic composition of this dust flux is estimated in this study using the small dataset presented for Atlantic aerosols. We thus assume that the leaching process used approximates true aerosol dissolution in the natural environment, and any associated isotopic fractionation. For Cu, the aerosol dataset has an average $\delta^{65}Cu = 0.00 \pm 0.18‰$ (1SD, $n = 6$), indistinguishable from the lithogenic value. Similarly, Zn isotopic data for Atlantic aerosols also have an average that is the same, within the uncertainties, as the lithogenic value (average $\delta^{66}Zn = +0.37 \pm 0.14‰$, 1SD, $n = 17$).

6.1.3. Summary of Cu and Zn inputs

Overall, the riverine dissolved flux of Cu is relatively well constrained, with three published estimates in the range 6–8.7 $\times 10^8$ mol/year (Boyle et al., 1977b; Gaillardet et al., 2003; Vance et al., 2008). The dust flux is more uncertain, particularly with regard to aerosol solubility, but is an order of magnitude lower than the riverine input. A factor of two increase in the value assigned to the dust flux would increase the total Cu input by <10%, within error of the estimated riverine flux. The residence time of Cu in the oceans, as estimated using the combined input flux of 7.7×10^8 mol/year Cu, and total Cu inventory of 4.2×10^{12} moles (assuming an average Cu concentration of 3.1 nmol kg^{-1}), is 5400 years (Table 4). This is similar to a previously published estimate by Boyle et al. (1977b), who report a residence time for Cu of 5000 years (using different boundary conditions).

The estimated Cu isotopic composition of this input flux is $\delta^{65}Cu = +0.63‰$ (Table 4). This value is dominated by the discharge-weighted isotope ratio for rivers estimated in Vance et al. (2008), at $\delta^{65}Cu = +0.68‰$, due to the relatively minor aerosol Cu source. The very limited dataset for aerosol dust reported in this study finds a $\delta^{65}Cu$ for dust unfractionated from the composition of upper continental crust, at $\delta^{65}Cu = 0.00‰$. Any significant increase in the magnitude of the dust flux would drive the Cu isotopic composition of the input towards lighter values. A factor of two increase in the dust flux reduces the projected Cu isotopic composition of the input by less than 0.05‰ however, to +0.59‰. The important aspect of this result for the overall purpose of this paper is that any estimate for the input of Cu (at somewhere between $\delta^{65}Cu = 0$ and 0.7‰, and a best estimate of +0.63‰) is distinctly lighter than the data so far obtained for the dissolved pool in the oceans. Specifically, three studies have found that the $\delta^{65}Cu$ of the dissolved pool in the deep oceans – in the Atlantic, Indian and Pacific Oceans – is heavier than these inputs at around $\delta^{65}Cu = +0.9 \pm 0.3‰$ (Vance et al., 2008; Boyle et al., 2012; Thompson et al., 2013), implying isotopic fractionation of Cu in the marine realm, and an output that preferentially removes the light isotopes of Cu.

Two estimates of the riverine flux of Zn differ by a factor of two, at 3.5 and 8.3 $\times 10^8$ mol/year (Gaillardet et al., 2003, this study). The midpoint of these two estimates is chosen as the 'best estimate' of the riverine Zn flux in Table 5. The estimated Zn dust flux is an order of magnitude lower than the riverine flux, at 6.9×10^7 mol year^{-1} Zn, resulting in a combined Zn input flux of 6.6×10^8 mol/year. Given an average oceanic Zn concentration of 5.4 nmol/kg (Chester and Jickells, 2012), this Zn input flux results in an oceanic residence time of 11,000 years, within the range of previous estimates (5000–50,000 years; Bruland, 1980; Shiller and Boyle, 1985; Bruland et al., 1994).

In contrast to Cu, the overall Zn input to the ocean must be very close to the lithogenic δ^{66}Zn value, with all three indicators of this input (rocks, rivers, and Atlantic dust) having average values within a very narrow range of δ^{66}Zn = +0.31 to +0.37‰. Our best estimate for the isotopic composition of the Zn input is δ^{66}Zn = +0.33‰ (Table 5). Published data for the Zn isotopic composition of the dissolved phase of seawater are, like Cu, scarce, but 6 depth profiles for the equatorial Atlantic (Boyle et al., 2012), Southern Ocean (Zhao et al., in press) and NE Pacific (Vance et al., 2012) demonstrate that the deep ocean (beneath 1000 m) has a strikingly uniform isotopic composition (δ^{66}Zn = 0.52 ± 0.02‰, 2SE, n = 26) that is slightly heavier than the inputs. This, then, also implies marine fractionation of Zn isotopes and, though in this case it is less extreme, this finding also requires an oceanic sink that is isotopically light for Zn.

6.2. The oxic output of Cu and Zn from the oceans, as recorded in Fe–Mn crusts

This study, compiling published and new data, has confirmed that there is fractionation of Cu and Zn isotopes during marine cycling, as suggested previously for Cu by Vance et al. (2008). Specifically, the inputs of Cu and Zn are isotopically light compared to the dissolved phase in seawater. Assuming steady state, this observation requires an isotopically light sink for Cu and Zn in ocean sediments. One possibility is a sink from oxic seawater, a large part of which is the result of Cu and Zn sorption on Fe–Mn oxides. We thus present Cu and Zn isotope data for Fe–Mn crusts as a proxy for this 'oxic' sink. Our results for the Cu and Zn isotopic compositions of Fe–Mn crusts are identical to those for Fe–Mn nodules obtained by Maréchal et al. (2000) and Albarède (2004). We find average Cu isotope values of δ^{65}Cu = +0.33‰ in an Atlantic Fe–Mn crust and δ^{65}Cu = +0.54‰ in the Pacific, both of which are isotopically lighter than reported values for the Cu isotopic composition of seawater (at δ^{65}Cu = ~0.9‰), as required for the marine fractionation of Cu isotopes. However, we find Zn isotope values that are isotopically heavier than deep seawater, with a homogenous average Zn isotope composition of all Fe–Mn crusts of δ^{66}Zn = +1.04‰.

The quantitative significance of these results depends on the magnitude of the output of Cu and Zn from the oceans in association with Fe–Mn oxides. By analogy with Mo, it is possible to make a first order estimate of the magnitude of this sink. Morford and Emerson (1999) estimate a total oxic sink for Mo of 9×10^7 mol/year, accounting for approximately half of the total Mo removal from the oceans. Assuming similar behaviour to Mo we estimate the size of the Cu and Zn oxic output using Cu/Mo and Zn/Mo ratios for Fe–Mn crusts. The average Cu/Mo ratio for the three Fe–Mn crusts in this study is 1.9 (by weight). The global average from a USGS compilation of over 600 published Fe–Mn crusts is higher, at 3.6 (Manheim and Lane-Bostwick, 1991). The value for Zn/Mo in our three Fe–Mn crusts is 1.2, compared to 2.4 for the USGS compilation. Using the values from the large USGS dataset, we estimate oxic removal of Cu to be 4.9×10^8 mol/year, and for Zn to be 3.1×10^8 mol/year (see Tables 4 and 5). For comparison, we estimate Zn removal in association with biogenic carbonates to be just $\sim 0.33 \times 10^8$ mol/year, assuming a global carbonate burial flux of 11×10^{12} mol/year (Milliman et al., 1999), and a Zn/Ca ratio of marine carbonates of 3 μmol Zn/mol Ca (Marchitto et al., 2000). In Tables 4 and 5 (and outlined in Section 6.1), we estimate the total input of Cu to the oceans to be $6.5–9.2 \times 10^8$ mol/year, and that of Zn to be $4.2–9.0 \times 10^8$ mol/year. These figures imply that oxic removal in association with Fe–Mn oxides removes about one half to two thirds of the total Cu and Zn input from the oceans each year. Thus, the flux mass balance of both Cu and Zn, as presented here, are out of balance, with significant sinks still to be identified. Note that, for the purposes of calculating the overall oceanic mass balance of Cu and Zn in Tables 4 and 5, we use the Fe–Mn nodule averages of Albarède (2004) for Cu (δ^{65}Cu = +0.31‰) and Maréchal et al. (2000) for Zn (δ^{66}Zn = +0.90‰), due to the global distribution of their large dataset (see Fig. 5).

6.3. The magnitude and isotopic composition of the missing sinks of Cu and Zn

Evidently, Fe–Mn oxides do not represent the sole output of Cu and Zn from the oceans. Missing sinks likely include settings associated with sedimentary sulphide, like the Black Sea, and in sinking particulate organic matter, such as in upwelling continental margins. Additional conclusions on the cycling of Cu and Zn isotopes in the ocean await these new datasets. However, an estimate of the size and isotopic composition of the missing sink for each element can be estimated from Eq. (7).

For Cu, an isotopically heavy missing sink of 2.8×10^8 mol/year with δ^{65}Cu = +1.2‰ is predicted (Table 4). However, the isotopic composition of the missing sink is sensitive to its magnitude (i.e. to the difference between the known input and output fluxes). Increasing the magnitude of the missing Cu sink, for example by increasing the size of the input flux, renders it isotopically lighter. This is illustrated in Fig. 6. Returning to the analogy with Mo, the standing pool of Mo in seawater is isotopically heavy due to preferential removal of light isotopes into Fe–Mn oxides (Siebert et al., 2003). The oceanic mass balance Mo is then closed by the removal of heavy Mo isotopes in marginal and euxinic settings, with quantitative removal in the latter (e.g. Black Sea) (Anbar and Rouxel, 2007). Similarly, this study has illustrated that the accumulation of light isotopes of Cu in Fe–Mn oxides might provide the isotopically light sink required by the observed fractionation of Cu isotopes in the marine realm. In addition, and also like Mo, Cu is strongly stripped out of the water column of the Black Sea and correspondingly enriched in sediments (Calvert and Pedersen, 1993). This setting thus provides one possible sink for heavy Cu isotopes, if quantitative removal results in the preservation of the seawater Cu isotopic composition (at δ^{65}Cu = ~0.9‰) in euxinic sediments.

The heaviest δ^{65}Cu value for a lithogenic sediment sample measured to date is +0.35‰, for Atlantic sediment

trap material (Maréchal et al., 1999). Biological processes appear to concentrate light isotopes of Cu (Zhu et al., 2010; Navarrete et al., 2011; Weinstein et al., 2011). Sorption processes on Fe oxy(hydr)oxide and organic surfaces tend to favour accumulation of heavy Cu isotopes (Balistrieri et al., 2008; Pokrovsky et al., 2008; Navarrete et al., 2011); to date the largest Δ^{65}Cu sorption fractionation measured is +1.25‰ (for gibbsite; Pokrovsky et al., 2008). Redox processes lead to large variations in δ^{65}Cu, with both heavy and light values (range: −0.48 to +1.17‰) reported as a result of Cu cycling in and around hydrothermal vents (Zhu et al., 2002), and an even larger range in the products of secondary mineralisation (Mathur et al., 2009).

The sensitivity of the predicted missing Zn sink to changing the magnitude of the Zn input flux is illustrated in Fig. 6. For the 'best estimate' presented in this study, this projected missing sink has a flux of 3.1×10^8 mol/year, and a light isotopic composition of $\delta^{66}Zn = -0.3$‰ (Table 5). The Zn isotopic composition of seawater (at $\delta^{66}Zn = \sim 0.5$‰), which is isotopically heavy compared to the postulated detrital Zn input (Table 5), also requires intra-oceanic removal of light Zn isotopes. The most obvious possible sink for light Zn is uptake and burial in organic matter. Cellular uptake of Zn by diatoms has an associated Zn isotopic fractionation of $\Delta^{66}Zn_{diatom\text{-}media}$ of −0.2‰ to −0.8‰ (John et al., 2007a), and Peel et al. (2009) observe seasonal cycles in the δ^{66}Zn of sediment trap material in a productive lake in Switzerland, with the most negative values (of $\delta^{66}Zn = -0.66 \pm 0.08$‰) associated with high summer productivity and large organic carbon fluxes. To date, however, very few light δ^{66}Zn values have been measured. Fe–Mn crust δ^{66}Zn values reported in this study are not dissimilar to those for other types of authigenic marine sediment that have been measured to date, including Fe–Mn nodules ($\delta^{66}Zn = 0.90 \pm 0.28$‰; Maréchal et al., 2000), biogenic carbonates ($\delta^{66}Zn = 0.91 \pm 0.24$‰; Pichat et al., 2003), and biogenic opal ($\delta^{66}Zn = 0.76$–1.47‰; Andersen et al., 2011). In the most comprehensive study of Zn isotopes in sediments to date, Maréchal et al. (2000) find that, excepting their data for ferromanganese nodules and two heavy values for carbonate- and opal-dominated samples (at $\delta^{66}Zn = 0.79$ and 0.69‰ respectively), δ^{66}Zn ratios in a range of other sediment types appear to be unfractionated from the lithogenic Zn isotopic composition. Taken together, these data highlight the requirement for a light sink for Zn isotopes that has not yet been identified.

The preceding discussion of the nature and isotopic composition of the missing sinks of Cu and Zn is not intended to be comprehensive. It is meant simply as a starting point for discussion, and for future work. For example, for Zn, we do not discuss the possibility outlined by Pons et al. (2013) that the cycle is balanced by an additional isotopically heavy source of Zn brought to the ocean in the suspended load of rivers, and mobilised in estuaries (Pons et al., 2013). We emphasise that understanding the modern cycles of the novel transition metal isotopes is critical, because without it the application of Cu and Zn isotopes as tracers for past processes is severely limited.

ACKNOWLEDGEMENTS

The authors would like to thank Corey Archer, Cliff Buck, Gavin Foster, Nigel Harris, Jim Hein, Sune Nielsen, Alan Whittington and Lian Zhou for supplying some of the samples analysed here. Helpful discussion with Morten Andersen is gratefully acknowledged, as are the comments of three anonymous reviewers and the associate editor Mark Rehkämper. This work was supported by NERC studentship NE/H525111/1 to S.H.L. and NERC Grant NE/G009961/1 and a Leverhume Trust Fellowship to D.V.

APPENDIX A. SUPPLEMENTARY DATA

Supplementary data associated with this article can be found, in the online version, at http://dx.doi.org/10.1016/j.gca.2013.07.046.

REFERENCES

Ackroyd D., Bale A., Howland R., Knox S., Millward G. and Morris A. (1986) Distributions and behaviour of dissolved Cu, Zn and Mn in the Tamar Estuary. *Estuarine Coastal Shelf Sci.* **23**(5), 621–640.

Albarède F. (2004) The stable isotope geochemistry of copper and zinc. *Rev. Mineral. Geochem.* **55**(1), 409–427.

Algeo T. and Maynard J. (2008) Trace-metal covariation as a guide to water-mass conditions in ancient anoxic marine environments. *Geosphere* **4**(5), 872–887.

Anbar A. D. and Rouxel O. (2007) Metal stable isotopes in paleoceanography. *Annu. Rev. Earth Planet. Sci.* **35**, 717–746.

Andersen M., Vance D., Archer C., Anderson R., Ellwood M. and Allen C. (2011) The Zn abundance and isotopic composition of diatom frustules, a proxy for Zn availability in ocean surface seawater. *Earth Planet. Sci. Lett.* **301**(1), 137–145.

Archer C. and Vance D. (2004) Mass discrimination correction in multiple-collector plasma source mass spectrometry: an example using Cu and Zn isotopes. *J. Anal. At. Spectrom.* **19**(5), 656–665.

Archer C. and Vance D. (2008) The isotopic signature of the global riverine molybdenum flux and anoxia in the ancient oceans. *Nat. Geosci.* **1**(9), 597–600.

Asael D., Matthews A., Bar-Matthews M. and Halicz L. (2007) Copper isotope fractionation in sedimentary copper mineralization (Timna Valley, Israel). *Chem. Geol.* **243**(3–4), 238–254.

Balistrieri L. S., Borrok D. M., Wanty R. B. and Ridley W. I. (2008) Fractionation of Cu and Zn isotopes during adsorption onto amorphous Fe(III) oxyhydroxide: experimental mixing of acid rock drainage and ambient river water. *Geochim. Cosmochim. Acta* **72**(2), 311–328.

Balls P. (1990) Distribution and composition of suspended particulate material in the Clyde estuary and associated sea lochs. *Estuarine Coastal Shelf Sci.* **30**(5), 475–487.

Baumgartner A., Reichel E. and Lee R. (1975) The World Water Balance: Mean Annual Global, Continental and Maritime Precipitation, Evaporation and Run-off. Elsevier Scientific Publishing Company.

Beard B. L., Johnson C. M., Cox L., Sun H., Nealson K. H. and Aguilar C. (1999) Iron isotope biosignatures. *Science* **285**(5435), 1889–1892.

Benoit G., Oktay-Marshall S., Cantu A., Hood E., Coleman C., Corapcioglu M. and Santschi P. (1994) Partitioning of Cu, Pb, Ag, Zn, Fe, Al, and Mn between filter-retained particles, colloids, and solution in six Texas estuaries. *Mar. Chem.* **45**(4), 307–336.

Bermin J., Vance D., Archer C. and Statham P. J. (2006) The determination of the isotopic composition of Cu and Zn in seawater. *Chem. Geol.* **226**(3–4), 280–297.

Berner E. and Berner R. (1996) Global Environment: Water, Air, and Geochemical Cycles. Prentice-Hall. Inc., Upper Saddle River, NJ.

Boyd P. and Ellwood M. (2010) The biogeochemical cycle of iron in the ocean. *Nat. Geosci.* **3**(10), 675–682.

Boyle E., Edmond J. and Sholkovitz E. (1977a) The mechanism of iron removal in estuaries. *Geochim. Cosmochim. Acta* **41**(9), 1313–1324.

Boyle E., Huested S. and Grant B. (1982) The chemical mass balance of the Amazon Plume – II. Copper, nickel, and cadmium. *Deep Sea Res. Part A* **29**(11), 1355–1364.

Boyle E., John S., Abouchami W., Adkins J., Echegoyen-Sanz Y., Ellwood M., Flegal A., Fornace K., Gallon C. and Galer S., et al. (2012) GEOTRACES IC1 (BATS) contamination-prone trace element isotopes Cd, Fe, Pb, Zn, Cu, and Mo intercalibration. *Limnol. Oceanogr. Methods* **10**, 653–665.

Boyle E. A. (1981) Cadmium, zinc, copper, and barium in foraminifera tests. *Earth Planet. Sci. Lett.* **53**(1), 11–35.

Boyle E. A., Sclater F. R. and Edmond J. M. (1977b) Distribution of dissolved copper in the pacific. *Earth Planet. Sci. Lett.* **37**(1), 38–54.

Bruland K. and Franks (1983). , pp. 157–215. Ch. 45.

Bruland K. W. (1980) Oceanographic distributions of cadmium, zinc, nickel, and copper in the North Pacific. *Earth Planet. Sci. Lett.* **47**(2), 176–198.

Bruland K. W. (1989) Complexation of zinc by natural organic ligands in the Central North Pacific. *Limnol. Oceanogr.* **34**(2), 269–285.

Bruland K. W. and Lohan M. C. (2003) Controls of Trace Metals in Seawater. Pergamon, Oxford, pp. 23–47.

Bruland K. W., Orians K. J. and Cowen J. P. (1994) Reactive trace metals in the stratified central North Pacific. *Geochim. Cosmochim. Acta* **58**(15), 3171–3182.

Brumsack H. (2006) The trace metal content of recent organic carbon-rich sediments: implications for cretaceous black shale formation. *Palaeogeogr. Palaeoclimatol. Palaeoecol.* **232**(2), 344–361.

Buck C., Landing W. and Resing J., et al. (2010) The solubility and deposition of aerosol Fe and other trace elements in the north atlantic ocean: observations from the A16N CLIVAR/CO_2 repeat hydrography section. *Mar. Chem.* **120**(1), 57–70.

Buck K. N., Moffett J., Barbeau K. A., Bundy R. M., Kondo Y. and Wu J. (2012) The organic complexation of iron and copper: an intercomparison of competitive ligand exchange-adsorptive cathodic stripping voltammetry (CLE-ACSV) techniques. *Limnol. Oceanogr. Methods* **10**, 496–515.

Calvert S. (1990). *Geochemistry and origin of the Holocene sapropel in the Black Sea.* , pp. 326–352.

Calvert S. and Pedersen T. (1993) Geochemistry of recent oxic and anoxic marine sediments: implications for the geological record. *Mar. Geol.* **113**(1), 67–88.

Cave R. R., German C. R., Thomson J. and Nesbitt R. W. (2002) Fluxes to sediments underlying the Rainbow hydrothermal plume at 36 14 N on the Mid-Atlantic Ridge. *Geochim. Cosmochim. Acta* **66**(11), 1905–1923.

Chen J., Gaillardet J. and Louvat P. (2008) Zinc isotopes in the Seine River waters, France: a probe of anthropogenic contamination. *Environ. Sci. Technol.* **42**(17), 6494–6501.

Chen Y., Street J. and Paytan A. (2006) Comparison between pure-water- and seawater-soluble nutrient concentrations of aerosols from the Gulf of Aqaba. *Mar. Chem.* **101**(1), 141–152.

Chester R., Bradshaw G. and Corcoran P. (1994) Trace metal chemistry of the North Sea particulate aerosol; concentrations, sources and sea water fates. *Atmos. Environ.* **28**(17), 2873–2883.

Chester R. and Jickells T. (2012) *Marine Geochemistry*. Wiley-Blackwell.

Cloquet C., Carignan J. and Libourel G. (2006) Isotopic composition of Zn and Pb atmospheric depositions in an urban/periurban area of northeastern France. *Environ. Sci. Technol.* **40**(21), 6594–6600.

Coale K. H. and Bruland K. W. (1988) Copper complexation in the Northeast Pacific. *Limnol. Oceanogr.* **33**(5), 1084–1101.

Croot P. L., Moffett J. W. and Brand L. E. (2000) Production of extracellular Cu complexing ligands by eucaryotic phytoplankton in response to Cu stress. *Limnol. Oceanogr.* **45**(3), 619–627.

Croot P. L., Moffett J. W. and Luther G. W. (1999) Polarographic determination of half-wave potentials for copper-organic complexes in seawater. *Mar. Chem.* **67**(3–4), 219–232.

Desboeufs K., Sofikitis A., Losno R., Colin J. and Ausset P. (2005) Dissolution and solubility of trace metals from natural and anthropogenic aerosol particulate matter. *Chemosphere* **58**(2), 195–203.

Donat J. R. and Bruland K. W. (1990) A comparison of two voltammetric techniques for determining zinc speciation in Northeast Pacific Ocean waters. *Mar. Chem.* **28**(4), 301–323.

Duce R. A. and Tindale N. W. (1991) Atmospheric transport of iron and its deposition in the ocean. *Limnol. Oceanogr.*, 1715–1726.

Dupont C. L. and Ahner B. A. (2005) Effects of copper, cadmium, and zinc on the production and exudation of thiols by *Emiliania huxleyi*. *Limnol. Oceanogr.* **50**(2), 508–515.

Dupont C. L., Nelson R. K., Bashir S., Moffett J. W. and Ahner B. A. (2004) Novel copper-binding and nitrogen-rich thiols produced and exuded by *Emiliania huxleyi*. *Limnol. Oceanogr.* **49**(5), 1754–1762.

Edmond J., Spivack A., Grant B., Ming-Hui H., Sung C. and Zeng Xiushau C., et al. (1985) Chemical dynamics of the Changjiang estuary. *Cont. Shelf Res.* **4**(1), 17–36.

Elderfield H. and Schultz A. (1996) Mid-ocean ridge hydrothermal fluxes and the chemical composition of the ocean. *Annu. Rev. Earth Planet. Sci.* **24**, 191–224.

Ellwood M. J. and Van den Berg C. M. G. (2000) Zinc speciation in the Northeastern Atlantic Ocean. *Mar. Chem.* **68**(4), 295–306.

Feely R. A., Massoth G. J., Baker E. T., Gendron J. F., Paulson A. J. and Crecelius E. A. (1986) Seasonal and vertical variations in the elemental composition of suspended and settling particulate matter in Puget Sound, Washington. *Estuarine Coastal Shelf Sci.* **22**(2), 215–239.

Fischer A., Kroon J., Verburg T., Teunissen T. and Wolterbeek H. T. (2007) On the relevance of iron adsorption to container materials in small-volume experiments on iron marine chemistry: ^{55}Fe-aided assessment of capacity, affinity and kinetics. *Mar. Chem.* **107**(4), 533–546.

Fitzsimmons J. N. and Boyle E. A. (2012) An intercalibration between the GEOTRACES GO-FLO and the MITESS/Vanes sampling systems for dissolved iron concentration analyses (and a closer look at adsorption effects). *Limnol. Oceanogr. Methods* **10**, 437–450.

Francois R. (1988) A study on the regulation of the concentrations of some trace metals (Rb, Sr, Zn, Pb, Cu, V, Cr, Ni, Mn and Mo) in Saanich Inlet Sediments, British Columbia, Canada. *Mar. Geol.* **83**(1), 285–308.

Gaillardet J., Dupré B., Louvat P. and Allegre C. (1999) Global silicate weathering and CO_2 consumption rates deduced from the chemistry of large rivers. *Chem. Geol.* **159**(1), 3–30.

Gaillardet J., Viers J. and Dupré B. (2003) Trace elements in river waters. *Treatise Geochem.* **5**, 225–272.

Gehlen M., Heinze C. and Maier-Reimer E., et al. (2003) Coupled Al–Si geochemistry in an ocean general circulation model: a tool for the validation of oceanic dust deposition fields? *Global Biogeochem. Cycles* **17**(1), 1028.

German C. R., Campbell A. C. and Edmond J. M. (1991) Hydrothermal scavenging at the mid-Atlantic ridge: modification of trace element dissolved fluxes. *Earth Planet. Sci. Lett.* **107**(1), 101–114.

German C. R., Colley S., Palmer M. R., Khripounoff A. and Klinkhammer G. P. (2002) Hydrothermal plume-particle fluxes at 13 N on the East Pacific Rise. *Deep Sea Res. Part A* **49**(11), 1921–1940.

Gordon A. S., Donat J. R., Kango R. A., Dyer B. J. and Stuart L. M. (2000) Dissolved copper-complexing ligands in cultures of marine bacteria and estuarine water. *Mar. Chem.* **70**(1–3), 149–160.

Hand J., Mahowald N., Chen Y., Siefert R., Luo C., Subramaniam A. and Fung I. (2004) Estimates of atmospheric-processed soluble iron from observations and a global mineral aerosol model: biogeochemical implications. *J. Geophys. Res.* **109**(D17), D17205.

Haraldsson C. and Westerlund S. (1991) *Total and Suspended Cadmium, Cobalt, Copper, Iron, Lead, Manganese, Nickel and Zinc in the Water Column of the Black Sea*. Kluwer Academic Pub., pp. 161–172.

Hein J. R., Koschinsky A., Halbach P., Manheim F. T., Bau M., Kang J.-K. and Lubick N. (1997) Iron and manganese oxide mineralization in the Pacific. *Manganese mineralization: geochemistry and mineralogy of terrestrial and marine deposits* **119**, 123–138.

Helz G., Bura-Nakić E., Mikac N. and Ciglenečki I. (2011) New model for molybdenum behavior in euxinic waters. *Chem. Geol.* **284**(3), 323–332.

Jacobs L., Emerson S. and Huested S. (1987) Trace metal geochemistry in the Cariaco Trench. *Deep Sea Res. Part A* **34**(5), 965–981.

Jacobs L., Emerson S. and Skei J. (1985) Partitioning and transport of metals across the O2H2S interface in a permanently anoxic basin: Framvaren Fjord, Norway. *Geochim. Cosmochim. Acta* **49**(6), 1433–1444.

Jickells T., An Z., Andersen K. K., Baker A., Bergametti G., Brooks N., Cao J., Boyd P., Duce R. and Hunter K., et al. (2005) Global iron connections between desert dust, ocean biogeochemistry, and climate. *Science* **308**(5718), 67–71.

Jickells T. D. and Spokes L. J. (2001) Atmospheric iron inputs to the oceans. *IUPAC series on analytical and physical chemistry of environmental systems* **7**, 85–122.

John S., Geis R., Saito M. and Boyle E. (2007a) Zinc isotope fractionation during high-affinity and low-affinity zinc transport by the marine diatom *Thalassiosira oceanica*. *Limnol. Oceanogr.*, 2710–2714.

John S., Rouxel O., Craddock P., Engwall A. and Boyle E. (2008) Zinc stable isotopes in seafloor hydrothermal vent fluids and chimneys. *Earth Planet. Sci. Lett.* **269**(1), 17–28.

John S. G., Genevieve Park J., Zhang Z. and Boyle E. A. (2007b) The isotopic composition of some common forms of anthropogenic zinc. *Chem. Geol.* **245**(1), 61–69.

Jones B. and Turki A. (1997) Distribution and speciation of heavy metals in surficial sediments from the Tees Estuary, north-east England. *Mar. Pollut. Bull.* **34**(10), 768–779.

Juillot F., Maréchal C., Ponthieu M., Cacaly S., Morin G., Benedetti M., Hazemann J., Proux O. and Guyot F. (2008) Zn isotopic fractionation caused by sorption on goethite and 2-lines ferrihydrite. *Geochim. Cosmochim. Acta* **72**(19), 4886–4900.

Kohfeld K. E. and Harrison S. P. (2001) DIRTMAP: the geological record of dust. *Earth Sci. Rev.* **54**(1), 81–114.

Koschinsky A. and Hein J. (2003) Uptake of elements from seawater by ferromanganese crusts: solid-phase associations and seawater speciation. *Mar. Geol.* **198**(3), 331–351.

Kraepiel A. M., Chiffoleau J.-F., Martin J.-M. and Morel F. M. (1997) Geochemistry of trace metals in the Gironde estuary. *Geochim. Cosmochim. Acta* **61**(7), 1421–1436.

Leal M. F. C., Vasconcelos M. and Van den Berg C. M. G. (1999) Copper-induced release of complexing ligands similar to thiols by *Emiliania huxleyi* in seawater cultures. *Limnol. Oceanogr.* **44**(7), 1750–1762.

Ling H. F., Burton K. W., Onions R. K., Kamber B. S., von Blanckenburg F., Gibb A. J. and Hein J. R. (1997) Evolution of Nd and Pb isotopes in Central Pacific seawater from ferromanganese crusts. *Earth Planet. Sci. Lett.* **146**(1–2), 1–12.

Lohan M. C., Statham P. J. and Crawford D. W. (2002) Total dissolved zinc in the upper water column of the subarctic North East Pacific. *Deep-Sea Res. Part A* **49**(24–25), 5793–5808.

Mahowald N. M., Baker A. R., Bergametti G., Brooks N., Duce R. A., Jickells T. D., Kubilay N., Prospero J. M. and Tegen I. (2005) Atmospheric global dust cycle and iron inputs to the ocean. *Global Biogeochem. Cycles* **19**(4), GB4025.

Manheim F. and Lane-Bostwick C. (1991) Chemical composition of ferromanganese crusts in the world ocean: a review and comprehensive chemical composition of ferromanganese crusts in the world ocean: a review and comprehensive database. Open-File Report 89-020, U.S. Geological Survey, Woods Hole, MA.

Marchitto, Jr., Thomas M., Curry W. B. and Oppo D. W. (2000) Zinc concentrations in benthic foraminifera reflect seawater chemistry. *Paleoceanography* **15**(3), 299–306.

Maréchal C., Nicolas E., Douchet C. and Albarède F. (2000) Abundance of zinc isotopes as a marine biogeochemical tracer. *Geochem. Geophys. Geosyst.* **1**(5), 1015–15.

Maréchal C. N., Telouk P. and Albarède F. (1999) Precise analysis of copper and zinc isotopic compositions by plasma-source mass spectrometry. *Chem. Geol.* **156**(1–4), 251–273.

Martin J. H., Fitzwater S. E., Michael Gordon R., Hunter C. N. and Tanner S. J. (1993) Iron, primary production and carbon–nitrogen flux studies during the JGOFS North Atlantic bloom experiment. *Mar. Chem.* **40**(1–2), 115–134.

Mason T. F., Weiss D. J., Horstwood M., Parrish R. R., Russell S. S., Mullane E. and Coles B. J. (2004) High-precision Cu and Zn isotope analysis by plasma source mass spectrometry. Part 2. Correcting for mass discrimination effects. *J. Anal. At. Spectrom.* **19**(2), 218–226.

Mathur R., Titley S., Barra F., Brantley S., Wilson M., Phillips A., Munizaga F., Maksaev V., Vervoort J. and Hart G. (2009) Exploration potential of Cu isotope fractionation in porphyry copper deposits. *J. Geochem. Explor.* **102**(1), 1–6.

McManus J., Berelson W., Severmann S., Poulson R., Hammond D., Klinkhammer G. and Holm C. (2006) Molybdenum and uranium geochemistry in continental margin sediments: paleoproxy potential. *Geochim. Cosmochim. Acta* **70**(18), 4643–4662.

Measures C. and Vink S. (2000) On the use of dissolved aluminum in surface waters to estimate dust deposition to the ocean (paper 1999gb001188). *Global Biogeochem. Cycles* **14**(1), 317–328.

Milliman J., Troy P., Balch W., Adams A., Li Y.-H. and Mackenzie F. (1999) Biologically mediated dissolution of calcium carbonate above the chemical lysocline? *Deep Sea Res. Part I* **46**(10), 1653–1669.

Moffett J. W. and Brand L. E. (1996) Production of strong, extracellular Cu chelators by marine cyanobacteria in response to Cu stress. *Limnol. Oceanogr.* **41**(3), 388–395.

Moffett J. W. and Dupont C. (2007) Cu complexation by organic ligands in the sub-arctic NW Pacific and Bering Sea. *Deep Sea Res. Part I* **54**(4), 586–595.

Morel F. M. M. and Price N. M. (2003) The biogeochemical cycles of trace metals in the oceans. *Science* **300**(5621), 944–947.

Morford J. and Emerson S. (1999) The geochemistry of redox sensitive trace metals in sediments. *Geochim. Cosmochim. Acta* **63**(11), 1735–1750.

Nägler T., Neubert N., Böttcher M., Dellwig O. and Schnetger B. (2011) Molybdenum isotope fractionation in pelagic euxinia: evidence from the modern Black and Baltic Seas. *Chem. Geol.* **289**(1), 1–11.

Nakagawa Y., Takano S., Firdaus M., Norisuye K., Hirata T., Vance D. and Sohrin Y. (2012) The molybdenum isotopic composition of the modern ocean. *Geochem. J.* **46**(2), 131.

Navarrete J., Borrok D., Viveros M. and Ellzey J. (2011) Copper isotope fractionation during surface adsorption and intracellular incorporation by bacteria. *Geochim. Cosmochim. Acta* **75**(3), 784–799.

Nriagu J. and Pacyna J., et al. (1988) Quantitative assessment of worldwide contamination of air, water and soils by trace metals. *Nature* **333**(6169), 134–139.

O'Nions R. K., Frank M., Von Blanckenburg F. and Ling H. (1998) Secular variation of Nd and Pb isotopes in ferromanganese crusts from the Atlantic, Indian and Pacific Oceans. *Earth Planet. Sci. Lett.* **155**(1), 15–28.

Peel K., Weiss D. and Sigg L. (2009) Zinc isotope composition of settling particles as a proxy for biogeochemical processes in lakes: insights from the eutrophic Lake Greifen, Switzerland. *Limnol. Oceanogr.* **54**(5), 1699.

Peterson D., Cayan D., DiLeo J., Noble M. and Dettinger M. (1995) The role of climate in estuarine variability. *American Scientist; (United States)* **83**(1).

Pichat S., Douchet C. and Albarède F. (2003) Zinc isotope variations in deep-sea carbonates from the eastern equatorial Pacific over the last 175 ka. *Earth Planet. Sci. Lett.* **210**(1), 167–178.

Pokrovsky O., Viers J. and Freydier R. (2005) Zinc stable isotope fractionation during its adsorption on oxides and hydroxides. *J. Colloid Interface Sci.* **291**(1), 192–200.

Pokrovsky O. S., Vim J., Emnova E. E., Kompantseva E. I. and Freydier R. (2008) Copper isotope fractionation during its interaction with soil and aquatic microorganisms and metal oxy(hydr) oxides: possible structural control. *Geochim. Cosmochim. Acta* **72**(7), 1742–1757.

Pons M.-L., Fujii T., Rosing M., Quitté G., Télouk P. and Albarède F. (2013) A Zn isotope perspective on the rise of continents. *Geobiology*.

Pontér C., Ingri J., Burman J. and Boström K. (1990) Temporal variations in dissolved and suspended iron and manganese in the Kalix River, northern Sweden. *Chem. Geol.* **81**(1), 121–131.

Poulson R. L., Siebert C., McManus J. and Berelson W. (2006) Authigenic molybdenum isotope signatures in marine sediments. *Geology* **34**(8), 617–620.

Poulson-Brucker R., McManus J., Severmann S. and Berelson W. (2009) Molybdenum behavior during early diagenesis: insights from Mo isotopes. *Geochem. Geophys. Geosyst.* **10**(6), Q06010.

Poulton S. and Raiswell R. (2002) The low-temperature geochemical cycle of iron: from continental fluxes to marine sediment deposition. *Am. J. Sci.* **302**(9), 774–805.

Prospero J. M., Ginoux P., Torres O., Nicholson S. E. and Gill T. E. (2002) Environmental characterization of global sources of atmospheric soil dust identified with the Nimbus 7 Total Ozone Mapping Spectrometer (TOMS) absorbing aerosol product. *Rev. Geophys.* **40**(1), 1002.

Raiswell R. and Canfield D. (2012) The iron biogeochemical cycle past and present. *Geochem. Perspect.* **1**(1), 1–220.

Rehkamper M. and Nielsen S. (2004) The mass balance of dissolved thallium in the oceans. *Mar. Chem.* **85**(3), 125–139.

Rudnick R. and Gao S. (2003) Composition of the continental crust. *Treatise Geochem.* **3**, 1–64.

Schlosser C. and Croot P. L. (2008) Application of cross-flow filtration for determining the solubility of iron species in open ocean seawater. *Limnol. Oceanogr. Methods* **6**, 630–642.

Scott C. and Lyons T. (2012) Contrasting molybdenum cycling and isotopic properties in euxinic versus non-euxinic sediments and sedimentary rocks: refining the paleoproxies. *Chem. Geol.*, 19–27.

Shiller A. M. and Boyle E. (1985) Dissolved zinc in rivers. *Nature* **317**(6032), 49–52.

Shimmield G. and Price N. (1986) The behaviour of molybdenum and manganese during early sediment diagenesis – offshore Baja California, Mexico. *Mar. Chem.* **19**(3), 261–280.

Siebert C., McManus J., Bice A., Poulson R. and Berelson W. (2006) Molybdenum isotope signatures in continental margin marine sediments. *Earth Planet. Sci. Lett.* **241**(3), 723–733.

Siebert C., Nägler T., von Blanckenburg F. and Kramers J. (2003) Molybdenum isotope records as a potential new proxy for paleoceanography. *Earth Planet. Sci. Lett.* **211**(1), 159–171.

Tang D., Warnken K. W. and Santschi P. H. (2002) Distribution and partitioning of trace metals (Cd, Cu, Ni, Pb, Zn) in Galveston Bay waters. *Mar. Chem.* **78**(1), 29–45.

Tankéré S. P. C., Muller F. L. L., Burton J. D., Statham P. J., Guieu C. and Martin J. M. (2001) Trace metal distributions in shelf waters of the northwestern black sea. *Cont. Shelf Res.* **21**(13–14), 1501–1532.

Taylor S. and McLennan S. (1985). *The continental crust: its composition and evolution*.

Tegen I. and Fung I. (1995) Contribution to the atmospheric mineral aerosol load from land surface modification. *J. Geophys. Res.* **100**(D9), 18707–18718.

Thompson C. M., Ellwood M. J. and Will M. (2013) A solvent extraction technique for the isotopic measurement of dissolved copper in seawater. *Anal. Chim. Acta* **775**, 106–113.

Tipper E., Gaillardet J., Galy A., Louvat P., Bickle M. and Capmas F. (2010) Calcium isotope ratios in the world's largest rivers: a constraint on the maximum imbalance of oceanic calcium fluxes. *Global Biogeochem. Cycles* **24**(3).

Tipper E., Galy A., Gaillardet J., Bickle M., Elderfield H. and Carder E. (2006) The magnesium isotope budget of the modern ocean: constraints from riverine magnesium isotope ratios. *Earth Planet. Sci. Lett.* **250**(1), 241–253.

Tribovillard N., Algeo T., Lyons T. and Riboulleau A. (2006) Trace metals as paleoredox and paleoproductivity proxies: an update. *Chem. Geol.* **232**(1), 12–32.

Trocine R. P. and Trefry J. H. (1988) Distribution and chemistry of suspended particles from an active hydrothermal vent site on the Mid-Atlantic Ridge at 26 N. *Earth Planet. Sci. Lett.* **88**(1–2), 1–15.

Vance D., Archer C., Bermin J., Perkins J., Statham P. J., Lohan M. C., Ellwood M. J. and Mills R. A. (2008) The copper isotope geochemistry of rivers and the oceans. *Earth Planet. Sci. Lett.* **274**(1–2), 204–213.

Vance D., Zhao Y., Cullen J. T. and Lohan M. C. (2012) Zinc isotopic data from the NE Pacific reveals shallow recycling. *Mineral. Mag.* **76**, 2486.

Wang Z.-L. and Liu C.-Q. (2003) Distribution and partition behavior of heavy metals between dissolved and acid-soluble fractions along a salinity gradient in the Changjiang Estuary, eastern China. *Chem. Geol.* **202**(3), 383–396.

Wedepohl K. (1991) The composition of the upper earth's crust and the natural cycles of selected metals. metals in natural raw materials. In *Metals and their Compounds in the Environment. Occurrence, Analysis, and Biological Relevance*. VCH, New York, NY.

Weinstein C., Moynier F., Wang K., Paniello R., Foriel J., Catalano J. and Pichat S. (2011) Isotopic fractionation of Cu in plants. *Chem. Geol.* **286**(3), 266–271.

Windom H., Smith R., Rawlinson C., Hungspreugs M., Dharmvanij S. and Wattayakorn G. (1988) Trace metal transport in a tropical estuary. *Mar. Chem.* **24**(3), 293–305.

Yang R. and Van den Berg C. (2009) Metal complexation by humic substances in seawater. *Environ. Sci. Technol.* **43**(19), 7192–7197.

Zhao Y., Vance D., Abouchami W. and de Baar H. J. W. (in press) Zinc isotopes in the southern ocean – a tracer of biogeochemical cycling? *Geochim. Cosmochim. Acta*.

Zhu X., Li S., Luo Y. and Wu L. (2010) Copper isotopic fractionation by higher plants. *Geochim. Cosmochim. Acta Supp.* **74**, A1234.

Zhu X. K., Guo Y., Williams R. J. P., O'Nions R. K., Matthews A., Belshaw N. S., Canters G. W., de Waal E. C., Weser U., Burgess B. K. and Salvato B. (2002) Mass fractionation processes of transition metal isotopes. *Earth Planet. Sci. Lett.* **200**(1–2), 47–62.

Zhu X. K., O'Nions R. K., Guo Y., Belshaw N. S. and Rickard D. (2000) Determination of natural Cu-isotope variation by plasma-source mass spectrometry: implications for use as geochemical tracers. *Chem. Geol.* **163**(1–4), 139–149.

Zwolsman J. J., Van Eck B. and Van Der Weijden C. H. (1997) Geochemistry of dissolved trace metals (cadmium, copper, zinc) in the Scheldt estuary, southwestern Netherlands: impact of seasonal variability. *Geochim. Cosmochim. Acta* **61**(8), 1635–1652.

Associate editor: Mark Rehkamper